Performance and Wearability of Electronic and Infrared Stealth Textiles

by

Tiancheng Xu

A thesis

presented to the University of Waterloo

in fulfillment of the

thesis requirement for the degree of

Master of Applied Science

in

Electrical and Computer Engineering

Waterloo, Ontario, Canada, 2023

Author's Declaration

I hereby declare that I am the sole author of this thesis. This is a true copy of the thesis, including any required final revisions, as accepted by my examiners.

I understand that my thesis may be made electronically available to the public.

Abstract

The functionality of smart textiles continues to make progress, but its wearability is often not guaranteed at the same time. The rough and porous fabric surface, the added materials (eg. electronic materials) not possessing characteristics like breathability and drape, and inadequate research are the main reasons leading to this problem. In this work, two kinds of smart textiles, electronic textiles (e-textiles) and infrared stealth fabrics, are studied to improve their performance and ensure their wearability meanwhile. This work provides ideas and theoretical guidance for the development of these and similar smart textiles in the future.

Using thermoplastic polyurethane (TPU) film as an intermediate layer for printing e-textiles is very common as it provides a smooth surface for device deposition, leading to improved device performance. However, at the same time, the TPU interferes with many desirable properties of the fabric, which makes textiles less comfortable to wear. In order to reduce the impact of TPU film on the wearability of e-textiles, the effects of different TPU types and processing conditions on electronic textile properties are investigated for the first time. It is found that the increase of TPU film thickness can improve the electrical conductivity and stretchability of e-textiles. On the other hand, the drape, water vapor permeability (WVP) and thermal conductivity of textiles decreases. Lower density TPU types are better because they have improved WVP and heat transfer, while electrical conductivity and stretchability are unaffected. Compared to single-layered TPU films, double-layered TPU can greatly improve the electrical conductivity and stretchability of e-textiles because they have better deformation resistance and can isolate the conductive layer and the fabric, reducing the impact of the fabric on the conductive layer. Increasing the curing temperature can improve the electronic performance of the e-textiles, but higher temperatures cause the TPU films to melt and curl. Finally, increasing the laminating temperature and laminating time can effectively improve the electrical properties of e-textiles, but the

rigidity of e-textiles becomes larger. These results provide guidance to achieve a more seamless integration of electronics into textiles.

Due to the high surface roughness of fabric, most of the coatings that exert good infrared stealth performance on a flat substrate have greatly weakened performance on fabric. Worse still, these materials severely interfere with the original properties of fabrics after coating. To solve this problem, silver nanowires (AgNWs) are considered for the first time in the preparation of infrared stealth fabrics and found to be very suitable. First of all, due to its metallic characteristics, it can provide a low infrared emissivity for the coating. And compared with other forms of silver structures, it has the advantages of low gloss, fitting degree with fabric, and high transparency in the visible light region. In the optimization of AgNW parameters, it is found that AgNWs with smaller diameters have better infrared stealth effect. AgNW array agglomeration and arrangement phenomenon reduce the infrared stealthing performance of the coating. Adding resin to AgNW solution may better disperse AgNWs and reduce agglomeration and arrangement phenomenon. But the resin's absorption of infrared rays is also noteworthy. It is found that increasing curing time has no significant effect on the infrared reflectance of AgNW array but can improve the electrical conductivity of AgNW array. This shows that instead of electron movement between nanowires, the vibration of electrons in single nanowires determines their stealth properties.

Acknowledgements

First, I would like to express my gratitude to my parents, Changqing Xu and Hong Zhao, who have always expressed their support and love to me across the ocean. I couldn't have done this project without them. I would also like to thank all of my friends and family for their continued support.

I sincerely thank Professor Irene Goldthorpe for her guidance throughout my project. When I encounter obstacles and difficulties, she always gives me warm advice and support. At the same time, I would like to thank her for giving me the opportunity to cooperate with Alchemy.

I am thankful to my lab partners Muhammed Kayaharman, Jonathan Atkinson, Zhiqiao Yang, and Hubert Argasinski, for the academic discussions and the exchange of ideas.

Finally, I would like to acknowledge to Alchemy, the cooperation with them has allowed me to accumulate a lot of experience, and we have also left a deep friendship.

Table of Contents

List of Figures

Chapter 1

Introduction

1.1 Smart Textiles Overview

The function of textiles has long been beyond basic protection and warmth. Among the different kinds of textiles, there is a class of textiles that are specially designed to respond to external environments or stimuli. Such textiles are often referred to as smart textiles. More broadly, any textile that provides users with specialized properties or functions can be defined as a smart textile. At present, health monitoring, sports training, protective clothing, temperature management, location tracking, and many other functions are widespread smart textiles applications.

There are many ways to classify smart textiles. From a functional point of view, they can be divided into aesthetic smart textiles and high-performance smart textiles [1]. Aesthetic smart textiles that combine luminescent devices with textiles are common in fashion [2]. High-performance smart textiles are intended to provide users with performance enhancements in certain areas, which covers a wider range. For example, medical textiles can prevent bacterial and viral infections during surgery, while special sports clothing can have better sweat management and sports performance enhancement functions [3], [4].

The degree of intelligence is a more systematic classification method, which divides smart textiles into passive smart textiles, active smart textiles, and ultra-smart textiles [2]. Some studies also call them first, second and third generation smart textiles. Passive smart textiles can provide users with special functions passively. In other words, they can only sense the external environment. For example, antibacterial textiles coated with metals or metal oxides, and thermal insulation textiles containing aerogels can be classified as passive smart textiles [5], [6]. This type of textile has the least intelligence and cannot adjust its function according to changes in stimuli, so they are classified into the category of functional fabrics in some research.

Active smart textiles are more intelligent and can sense and react to environmental stimuli. Thermal regulated smart textiles made of phase-change materials can absorb or release heat according to the external environment, which can effectively improve the wearing comfort of clothes [7]. In contrast, the above-mentioned thermal insulation textiles can only play the role of heat preservation. In addition to phase change materials, some other materials that can change their properties under external stimuli are also often used to prepare active smart textiles. Chromic materials can change color in response to external stimuli, and shape-memory materials return to their previous shape at the activation temperature [8], [9].

Ultra-smart textiles can not only sense and react to external environments or stimuli, but also have responding and adopting features. This type of textile has the highest degree of intelligence, which always has electronic devices such as microprocessors, sensors, nanogenerators, and/or energy storage devices integrated into the textile. Therefore, it can be said that except for some electronic textiles (e-textiles) that only have simple functions such as heating, the scope of ultra-smart textiles is close to that of e-textiles. Functions like monitoring important human body indicators, textile displays, and flexible energy storage are popular and becoming research hotspots in ultra-smart textiles [10], [11], [12].

At present, the smart textile market is developing rapidly, reaching a value of nearly US$2.5 billion in 2021, and is expected to grow at a rate of 30% to US$9.3 billion in 2026 [13]. This shows people's expectations for increased functionality of textiles and their interest in new technologies. Smart textiles are not only widely used in professional fields (such as military and medical fields) but are gradually entering people's everyday lives. Although the biggest segment of the smart textile market is still protection and military, the fastest-growing segment is sports and health, which is expected to grow at a compound annua l growth rate (CAGR) of 32% through to 2026 [13].

In recent research, more and more smart textile prototypes with different functions have been developed and passed feasibility studies. In most cases, the requirements for a certain function of smart textiles can be realized by a variety of materials and preparation methods. For example, antibacterial textiles can be realized by adding inorganic antibacterial agents such as zinc oxide and silver nanoparticles, or organic antibacterial agents such as chitin and chitosan

[5], [14]. However, one of the biggest challenges the field faces is that additional functions of the smart textile and the original merits of the fabric (such as softness, drapability, breathability) cannot be guaranteed simultaneously. To achieve good functionality, many functional materials or complicated electronics must be added to the textile, undoubtedly damaging clothing comfort. Also, the potential safety issue of using these materials is worrying, especially in smart textiles that fit with human skin. Therefore, rather than developing smart textiles with different functions, it is more important to study materials and preparation methods to improve the functionality of smart textiles without compromising their comfort. E-textiles are currently the most advanced and intelligent smart textiles. And infrared stealth fabrics are often used in military and defense fields, the largest market for smart textiles [13]. It is these two technologies that will be considered in this thesis. The following sections will introduce these two representative smart textiles and point out specific issues limiting their development.

1.2 E-textiles

1.2.1 Overview

E-textiles are defined as smart textiles formed by combining electronic devices and fabrics. It enhances the functionality of textiles and the application range of electronic devices, providing the possibility for more convenient human-computer interaction. The history of e-textiles began in the 19th century with attempts to combine lights with textiles for fashion and entertainment applications [15]. More modern e-textiles emerged starting in the 1950s. At an exhibition called Body Covering held in 1968, a spacesuit with inflation and deflation, heating and cooling, and luminous functions was exhibited [16]. With people's demand for more convenient human-computer interaction, e-textiles are developing rapidly. In the past few decades, with the development and exploration of wearable electronic technology, e-textiles have been developing rapidly. E-textile devices such as displays [11], solar cells [17], and touch sensors [18] have been demonstrated, and some e-textiles with simpler functions, like the electric heating vest, have been commercialized. With the expansion and improvement of functions in the next several years, e-textiles will gradually move from the laboratory to the public.

1.2.2 Fabrication Methods

Approaches to fabricating early-stage e-textiles were to simply connect clothing, electronics, and power with cables. An example is the LifeShirt from VivoMetrics, which detects parameters such as the user's cardiorespiratory fitness and posture information [19]. Lifeshirt can capture and record physiological data in real time, which is often used in research studies [19]. However, the fabrics and electronic components were not well integrated, which has the disadvantages of heavy wearing, lack of comfort, unsightly appearance, and low washability. This has hindered its further development into a mass market. It is more like a highly integrated detection system but ignores the wearability of the clothing. When developing the next generation of e-textiles, the electronic functionality and wearability of clothing need to be guaranteed at the same time, which means electronic components and fabrics need better integration. Many novel approaches have been tried, among which the adoption of wireless data transmission methods and the development of electronic components based on fabrics are two important aspects.

Except for some e-textiles that only have simple functions such as heating and lighting, most e-textiles have active monitoring functions, and how to transmit data to users has become a big problem. This problem is especially serious in commercial e-textiles with multiple functions. The Lifeshirt mentioned above has a lot of wires connected to the data collector from different areas of the clothing, which greatly hinders the wearability of the clothing. In order to reduce the number of wires used in textiles, wireless transmission technology is widely used in e-textiles. It replaces most of the wires between clothing and electronic devices, therefore greatly improving the comfort of the user while wearing. Daminano et al. combined a knitted folded dipole antenna with a radio frequency identification (RFID) chip to prepare a wireless and wearable strain sensor [20]. There are no wires on the prepared clothes, and the data of the user's physical movement is transmitted wirelessly between the RFID chip and the reader, ensuring the flexibility of the clothes. At present, wireless transmission technology has been widely used in commercial e-textiles such as the Hexoskin fitness jacket and the Adidas heart rate monitoring sports bra [21]. Users can obtain the monitoring data in real time on their mobile

phones.

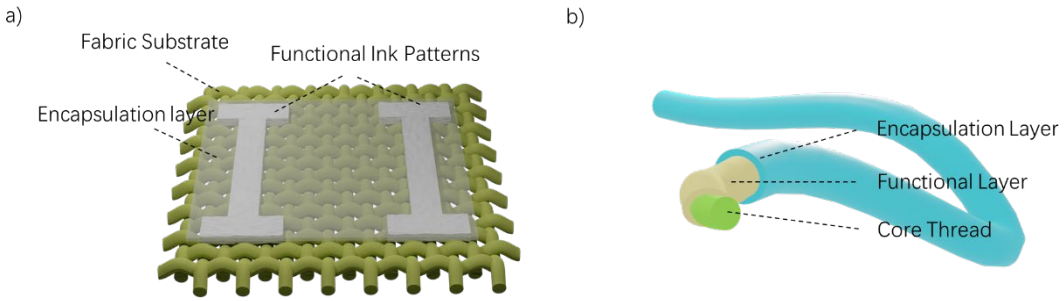

Figure 1-1: (a) Schematic diagram of fabric-based e-textiles. It usually consists of a fabric substrate, functional patterns printed by ink, and an encapsulation layer on top. (b) Schematic diagram of functional yarns. Fiber-based e-textiles are fabricated by integrating the functional yarns into a textile substrate and forming desired patterns.

The development of electronic components upon the fabric itself can significantly improve the flexibility and convenience of e-textiles since rigid substrates are not involved. It can be roughly divided into two preparation ideas: fabric-based (Figure 1-1 (a)) and fiber-based (Figure 1-1(b)); that is, preparing electronic components on the surface of fibers or fabrics.

When preparing fiber-based e-textiles, functional yarns are usually fabricated by coating functional materials on the surface of normal threads. Then the functional yarns are combined with the fabric by weaving [22], knitting [23], or embroidery [24] in a preset pattern to obtain functionalized fabric. Devices fabricated by this method, like electrodes [24], sensors [25], and antennas [26], have already been demonstrated in research, and there are many commercial e-textiles made by this method, such as Polar Bear heated garments and Google Jacquard jackets [21]. The problem with this method is that the weavability and knittability of the functional yarns are very limited since the mechanical properties of functional yarn differ from the traditional fiber. The tensile stress produced by the industrial textile machine on the yarn is about 2-4 MPa, which is likely to destroy the functionality of the yarn during the preparation process. This means that industrial machines have problems fabricating fiber-based e-textiles, which increases manufacturing costs. Applying an encapsulation layer on the surface of the yarn or using stainless steel spun threads as the core of the yarn could address this issue. However, the properties of the fabric will be altered, which means the comfort of the clothing is questionable.

Since the functionality of fiber-based e-textiles is often activated after the weaving process, device resolution is limited by the thickness of the yarn and the weaving method. Instead of a co-axial coating, some more advanced studies deposit miniaturized electronic components on the surface of yarns or flat filaments to increase resolution. For example, Adiodun et al. etched circuits on flexible filaments with a width of less than 2 mm and assembled LED strips [27]. The prepared filament is woven into the fabric to prepare e-textiles. Filaments with a relatively flat surface improve the preparation resolution and can contain fine circuits, microprocessors, and power supply equipment. The problem with this fabrication method is that the preparation process is very complicated. What is worse, the more delicate manipulation of the yarn means that the subsequent weaving process with the fabric is difficult.

Fabricating fabric-based e-textiles is more convenient than fiber-based. Functional inks, like conductive metal inks, are printed on the surface of the fabric to prepare devices and conductive paths. Techniques from the field of printed electronics are used, where electronics are 'printed' analogous to the way newspapers are printed, on alternative substrates like plastics and in this case textiles. Fabrication can be done at low temperatures, over large areas, and at low cost. Prototypes of many electronic devices, such as interconnections [28], electroluminescent lamps [29], and sensors [30], have been successfully printed on fabrics. Dispenser printing [29], screen printing [28], and inkjet printing [31] and are currently commonly used e-textile printing methods. Screen printing is the most popular one because it is already widely used in the textile industry and it is suitable for high-throughput, roll-to-roll production processes.

Figure 1-2 is a schematic of the screen printing process. The screen comprises a mesh with grid squares that are either open or closed to define the pattern (Figure 1-2 (a)). During printing, the screen printer is placed on the top of the substrate, and the squeegee moves across the screen to transfer the ink to the substrate (Figure 1-2 (b)). The closed mesh region (darker area of the screen) prevents the ink from touching the substrate while printing. The opened mesh region (brighter area of the screen) allows the ink to pass through, transferring the printed pattern. Figure 1-2 (c) is a schematic of the printed pattern, and one can see that the pattern is consistent with the shape of the opened mesh region. The use of printing technology to prepare e-textiles

can avoid the above-mentioned problems of the processability of the yarn and the complexity of the equipment used, thereby reducing preparation costs.

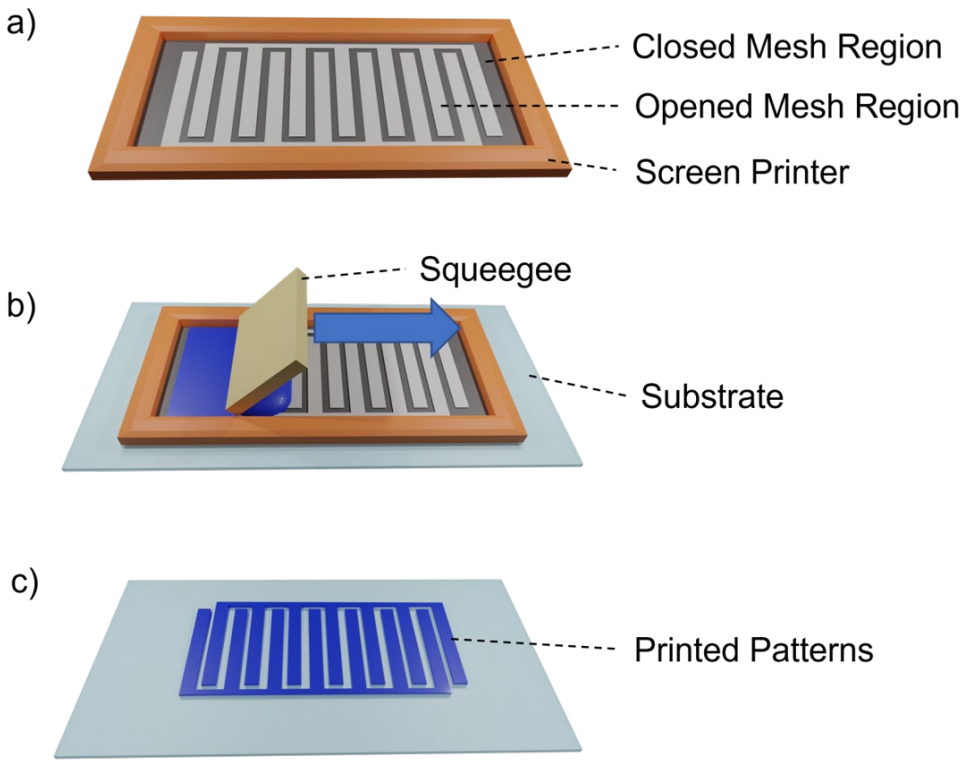

Figure 1-2: Schematic diagram of (a) a patterned screen, (b) the printing process, and (c) the resulting printed pattern.

To sum up, compared with fiber-based e-textiles, fabric-based e-textiles prepared by printing technology have advantages in terms of the ease of preparation, the convenience of the equipment used, and the integration with the current textile industry. The difficulties encountered in this method and related optimizations will be discussed below.

1.2.3 Limitations and Optimizations of Fabric-based E-textiles

Printed electronics most often use plastic films as the substrate. Printing on fabric is far more difficult due to the rough surface and porosity of the fabric substrates. This often leads to limited performance of the fabricated electronic devices, and as will be shown in Chapter 2, the

functionality of the devices further decreases when subjected to external stresses such as friction, stretching, and bending. Simply increasing the thickness of the functional ink will reduce the wearability of the textile severely as it increases stiffness, weight, and cost. The choice of fabric, the composition of ink components, and the use of additional intermediate layers are the three main optimization directions.

Choosing a suitable fabric is critical for subsequent print quality. Yongsang et al. printed circuit boards on fabrics and studied their electronic properties [32]. After comparing different fabrics, they stated that thicker fabric density and thinner yarns could improve the flatness of the fabric surface, thus improving the stability and reducing the resistance of the connection between the printed electronic device and the fabric. Starting from reducing the flatness of the fabric surface, Ying et al. chose nonwoven fabric as the substrate of e-textiles [33]. Nonwoven fabrics are directly bonded together by high-density fibers through physical methods, and there is no rough surface morphology woven by yarns, so they are better suited as printing substrates.

Changing the composition of functional substances or binders in printed ink can improve the ability of printed e-textiles to resist external pressure. When the fabric is stretched, the yarns parallel to the direction of stretching will elongate, and at the same time, the distance between the yarns perpendicular to the stretching direction will increase. These two aspects cause the uneven strain of the ink on the fabric as it undergoes stretching, which puts forward high requirements on the stretchability of the ink layer. Adding high-aspect-ratio conductive materials to the ink to ensure that the grains of the conductive material interconnect when stretched is a good idea. Therefore, materials such as nano-silver flakes [34], silver nanowires (AgNWs) [35], and carbon nanotubes (CNTs) [36] are often used in stretchable conductive inks. Changing the viscosity of ink to control the ink penetration depth is also an idea to improve printing quality. Yousef et al. printed a low-viscosity solution containing copper ions on the fabric [37]. The copper complex changed to copper atoms through self-reduction to form a conductive path. Due to the low viscosity of the solution, it can fully penetrate the fabric and form a conductive layer. The stretchability of the product is effectively improved because the conductive layer is closely connected to the fabric.

The above two optimization directions impose requirements on the types of fabrics and inks, which could limit the types of applications of e-textiles. For example, nonwoven fabric is less used in the field of durable clothing due to its poor durability and washability, and conductive inks with high-aspect-ratio materials have not been fully implemented in the market. In contrast, adding an intermediate layer on the surface of the fabric during printing does not require special fabrics or inks, which improves the application fields of e-textiles.

The use of the intermediate layer has many advantages. When the conductive ink is printed directly on the fabric, the ink surface is also rough due to the roughness of the substrate (Figure 1-3 (a)). This greatly reduces the resolution, performance, and mechanical properties of the printed device. The ink also seeps into the fabric requiring more ink to achieve a continuous layer. By printing the conductive ink on a smooth TPU intermediate layer first (Figure 1-3 (b)), then laminating the TPU-ink composite onto the fabric, the printing quality of the printed pattern is greatly improved (Figure 1-3 (c)). This is because the intermediate layer has an isolation effect and reduces the roughness of the fabric (Figure 1-3 (c)). A similar effect can also be achieved by pressing the TPU intermediate layer to the fabric first and then printing. Using a TPU intermediate layer makes conductive patterns have lower initial resistance and higher resolution. And because the roughness of the printing substrate is greatly reduced, the surface of the conductive layer is also smoother, which makes it possible to print more complex hierarchical structures later. For example, wearable textile displays is a hot topic in the field of e-textiles. However, due to the rough surface of the fabric, it is challenging to fabricate luminous devices on the fabric. At present, the more mature and popular fabrication method is still combining textile circuits with surface-mounted optical devices [38]. Feixiang et al. solved the problem by using a TPU intermediary layer [39]. Pictures from scanning electron microscope (SEM) show that the TPU film on the surface of the fabric effectively fills the gaps between the fibers, and the subsequent hierarchical structure is very smooth. The resulting device exhibits excellent brightness at lower voltages. Another advantage is the intermediate layer can improve the stretchability of the e-textiles since the conductive layer on a TPU film tends to be uniformly elongated when subjected to stretching. Sari et al. studied the tensile properties of conductive inks on different substrates [40]. They found that the resistance change

of a conductive layer on the polymer film substrate and the fabric substrate were very different. The conductive layer on the polymer film only has small cracks when it is stretched, but larger cracks are obvious when using fabrics as the substrate. Yokus et al. used screen printing to print Ag/AgCl conductive ink on TPU film and applied heat lamination to prepare fabric-TPU-conductive ink-TPU structured interconnects [41]. The printed interconnects prepared by this process can withstand a single strain of more than 100%, and a 20% strain cycled 1000 times.

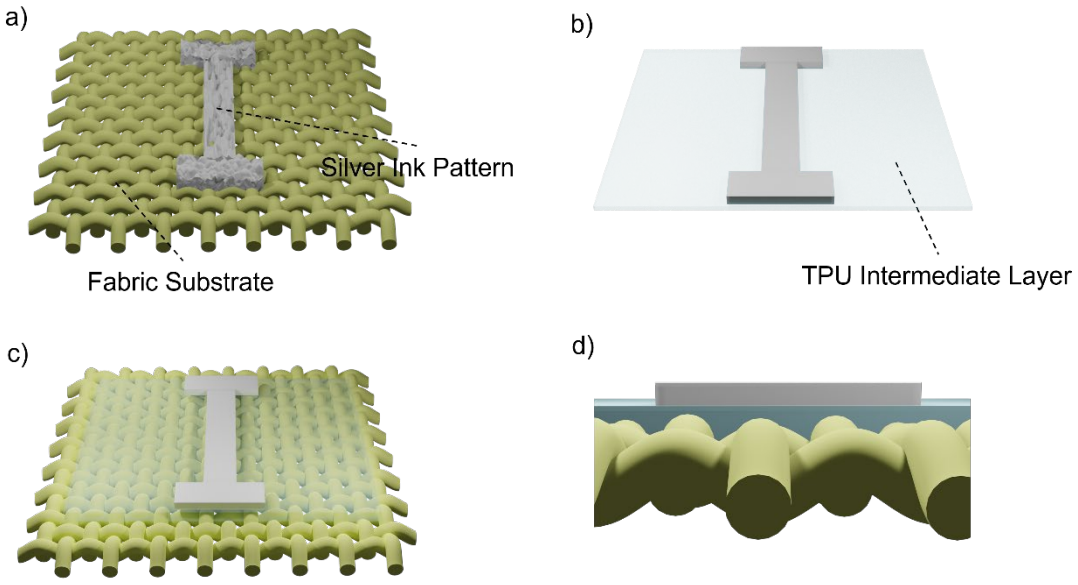

Figure 1-3: Schematics of printing directly on fabric versus the use of a TPU intermediary layer. (a) Direct printing of ink onto fabric. (b) - (d) The use of an intermediary layer: (b) Ink printed on TPU; (c) the TPU film is laminated onto fabric using heat and pressure; (d) the cross-section of the sample using an intermediary TPU layer.

The use of TPU has become a very common method of preparing e-textiles. However, although the intermediate layer brings large improvements in the device performance and cost of e-textiles, its mismatch with the modulus of the fabric and obstruction of the fabric's porosity reduces the comfort of human wearing. Therefore, it is crucial to optimize and adjust the TPU film and processing conditions so that e-textiles can better maintain the original advantages of the fabric, such as breathability and drape, while at the same time having good electronic properties. This will be the focus of study in Chapter 2.

1.3 Infrared Stealth Textiles

1.3.1 Stealth Technology

Stealth technology changes the observable information of an object to reduce the detection probability or the detectable distance. Stealth technology has a long history, such as turquoise paint used as camouflage for reconnaissance ships during the Gallic Wars of 56-54 BC [42]. With the continuous development of science and technology, the detectors in war upgraded from the naked eye and telescope to more advanced and multifunctional instruments such as radar, sonar, and infrared detectors. In order to improve the survivability of weapon systems and combat units, different stealth technologies have rapidly been developed. Correspondingly, stealth technologies have been developed for detectors with different principles. Generally, stealth technology can be divided into categories such as radar stealth, infrared stealth, laser stealth, acoustic and magnetic stealth, and visible light stealth. Because of the mature development and broad application scenarios of infrared and radar detection technology, their related stealth technology has become more prominent.

When detecting a target, radar radiates an electromagnetic wave and uses the reflection of that electromagnetic wave to discover the target and determine its position. Therefore, the essence of radar stealth technology is to reduce the radar scattering cross-sectional area (RCS) of the target so that radar cannot accurately detect the target echo signal. Two common radar stealth mechanisms are (i) using a unique shape design or absorbing material to reduce the reflected power or (ii) emitting a coherent but phase-opposite scattering field. Different from radar detection, the sensor used in infrared detection does not actively emit infrared but utilizes the passive infrared characteristics of the target for detection. Infrared stealth technology will be discussed in detail below.

1.3.2 The Mechanism of Infrared Stealth

To understand the mechanism of infrared stealth technology, it is necessary to first understand the principle of infrared detection. At present, point sources and imaging are the two

mainstream infrared detection methods [43]. The formula for the maximum working distance of a point source infrared detection system is:

$$R = \sqrt{\frac{D^* A_t A_0 \tau_a \tau_0 (L_t - L_b)}{N_t (A_d \Delta f)^{1/2} (V_s / V_N)}} \quad (1)$$

where R is the maximum working distance, D^* is the detection rate of the infrared detector, A_t is the target radiation area, A_0 is the entrance pupil area of the detection system, τ_a is the atmospheric transmittance at distance R, τ_0 is the optical transmittance of the infrared system, N_t is the number of pixels caused by dispersion, A_d is the area of the detector unit, Δf is the equivalent noise bandwidth of the amplifier circuit, V_s/V_N is the acceptable signal-to-noise ratio of the signal processor, L_b is the background radiance, and L_t is the target radiance. It can be seen that when the difference between the radiance of the target and that of the background is small or the radiation area of the target is small, the maximum operating distance is reduced.

An infrared imaging detector converts infrared radiation into electronic signals, and then the electronic signals are processed by the electronic processing system to display the infrared heat map. The imaging contrast ratio is defined as:

$$C = \frac{E_t - E_b}{E_b} \quad (2)$$

where C is the contrast ratio of the infrared imaging detector, E_t is the radiation energy density of the target, and E_b is the radiation energy density of the background. It also depends on the difference in the thermal radiation energy emitted by the background and the target.

Planck's black body radiation law (Formula 3) describes the spectral flux density of black bodies:

$$S(\lambda) = \frac{2\pi c^2 h}{\lambda^5} \frac{1}{e^{\frac{hc}{\lambda k T}} - 1} \quad (3)$$

where S is the spectral flux density of the black body, λ is the wavelength of light, h is the Plank constant, c is the speed of light, k is the Boltzmann constant, and T is the absolute temperature. By integrating Formula 3 over the wavelength and surface area and multiplying by the object's emissivity, the Stephen-Boltzmann law can be derived (Formula 4):

$$P = e\sigma A T^4 \quad (4)$$

where P is the radiant power of the object, e is the emissivity of the object, σ is the Stephen-Boltzmann constant, A is the surface area, and T is the object's temperature. This equation describes the radiant power of an object in a specific wavelength range as a function of temperature and emissivity. The temperature of the detected target is often higher than the ambient temperature, and the emissivity of the target without surface treatment is relatively high and close to 1. For example, the emissivity of polyester, cotton, and nylon fabric in the 8-12 μm range is around 0.88 [44]. Therefore, according to Formulas 1, 2, and 4, the radiant power of the detected target is often much greater than that of the background, so the infrared detector can easily detect the target.

The attenuation of infrared transmission through the atmosphere is also important in real-world infrared detection. Since the energy required for the vibration of molecules (e.g., CO_2, H_2O) is in the infrared range, these molecules in the atmosphere absorb infrared light. After deducing the infrared range that will be absorbed by the molecules in the atmosphere, three atmospheric windows in the infrared range that can allow infrared pass through atmosphere are the short-wavelength infrared (SWIR) range (1-2.5 μm), mid-wavelength infrared (MWIR) range (3-5 μm) and long-wavelength infrared (LWIR) range (8-12 μm). Therefore, most of the infrared detectors currently used are within these three ranges. According to Formula 3, the magnitude and distribution of the spectral flux density of objects at different temperatures are different. The higher the temperature, the shorter the wavelength of infrared radiation emitted by the object. It is vital to select the appropriate infrared sensor according to the temperature range of the detected target.

Through the exploration of the above principles of infrared detection, the following mainstream methods can be used to achieve infrared stealth:

1. Reducing the infrared radiation intensity difference between the detection target and the background. From Formulas 1, 2, and 4, this can be achieved by reducing the emissivity of the object surface and the temperature difference. Infrared stealth fabric often adopts this stealth idea. The low-emissivity or thermal insulated coating is covered on the surface of the fabric to achieve the effect of infrared stealthing. Reducing the surface area with high temperatures is also an effective way. Some military equipment such as aircraft, tanks can

achieve this by optimizing the design of the equipment structure [45].

2. Adjusting the infrared transmission path of the target, such as laying a smoke screen between the detected target and the infrared detector. The smoke screen has absorption, reflection, and scattering effects on the infrared rays emitted by the target, and the smoke screen itself can also emit infrared rays outward. These two aspects significantly weaken the difference between the thermal radiation energy of the target and the background, which leads to a good infrared stealth effect.
3. Changing the target infrared radiation wavelength range. For example, adding special additives to aircraft fuel can shift the emission of aircraft plumes to the 5-8 μm band [45]. The modified radiation wavelength band is just outside the effective range of the infrared detector, so infrared stealth is achieved.

1.3.3 Infrared Stealth Fabric

Figure 1-4 shows the variation curves of the spectral flux density of the human body (37 °C) and the surrounding background (20 °C) as a function of wavelength, assuming that the emissivity is unity. There is a considerable difference between the infrared radiation of the human body and the surrounding environment. Therefore, it is necessary to apply infrared stealth technology to fabrics. Figure 1-4 also explains why LWIR and MWIR thermal cameras instead of SWIR cameras are the two commonly used for detecting humans.

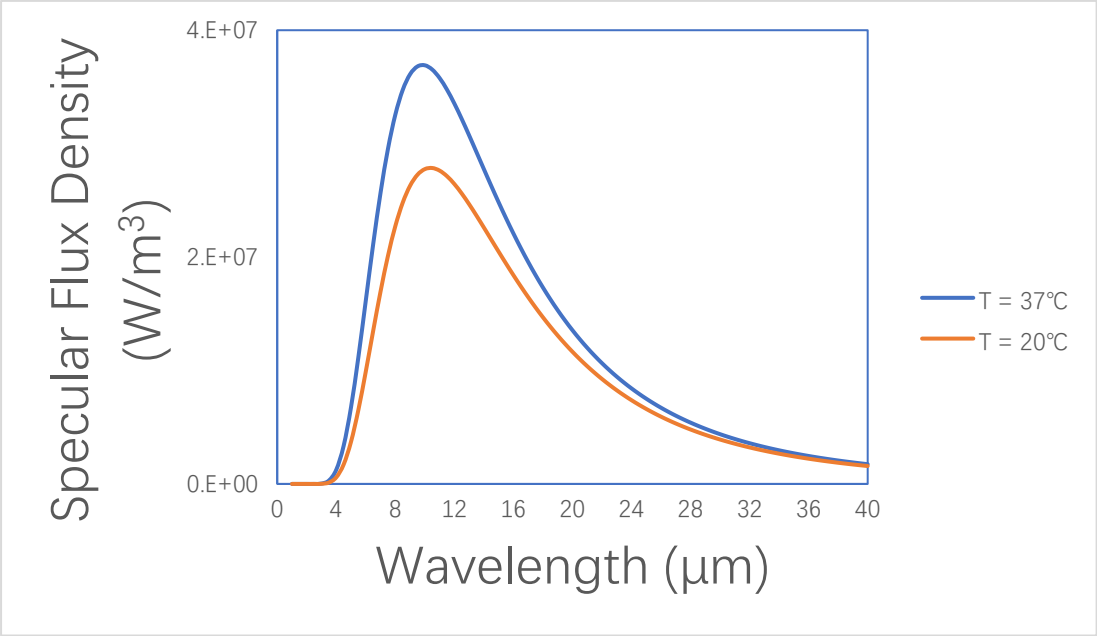

Figure 1-4: The simulated flux density of objects at 37 ℃ and 20 ℃. The simulation wavelength range is from 0 to 40 μm.

Since it is difficult to change the body temperature drastically, the focus of infrared stealth fabrics should be on thermal insulation and low emissivity coatings. The three main ways of heat transfer are heat conduction, heat radiation, and heat convection, so a good thermal insulation material should isolate heat from these three aspects. For example, aerogel is a solid material with a nanoporous network structure, and its porosity can reach 99% [46]. The heat transfer of aerogel materials mainly occurs through heat conduction and convection between gases, heat conduction through the solid skeleton, and heat radiation. Due to the nanoporous structure of aerogel, in which the free movement of gas is restricted, effective thermal convection cannot be formed. The flow of gas molecules in the aerogel is in the transition zone, or the free molecule zone, and the gas molecules collide elastically with the pore wall instead of colliding with other gas molecules to complete heat exchange. Hence, the thermal conductivity through gases is very low. Due to the nanoporous network structure of aerogel, the thermal conduction path is very long, so the thermal conductivity through the solid skeleton is also very low. The solid skeleton in the aerogel can effectively absorb, reflect, or refract energy when thermal radiation occurs, so the thermal radiation rate is very low. Aerogel can effectively prevent the above three heat transfer methods, so it is a good thermal insulation material.

When the infrared wave radiated from the human body is transmitted to the fabric, the wave could be transmitted, reflected, or absorbed. Assuming that transmissivity of fabric is 0, it can be obtained that absorptivity + reflectivity = 1. According to Kirchhoff's radiation law, for any object in thermodynamic equilibrium to emit and absorb thermal radiation, the emissivity is equal to the absorptivity [47]. Therefore, objects with high reflectivity have low emissivity and can often be used in infrared stealth fabrics, such as metal particles.

It is worth noting that in addition to emitting infrared light, the fabric also reflects the infrared light emitted by sunlight. A fabric surface that is too flat will specularly reflect the sun, which is easy to be detected by an infrared camera. Untreated fabrics rarely have this problem due to their surface roughness and thus mostly diffuse light. However, infrared stealth fabrics are often coated and have a smoother surface, so this type of problem is more severe. Thick coatings will also damage the original good flexibility, moisture permeability, and thermal conductivity of the fabric. Using only a small amount of paint to better maintain the roughness and original performance of the fabric surface while achieving good stealth performance is one key to development.

Since the fabric will inevitably undergo friction and repeating stretching during wearing, the robustness of the coating itself and the degree of matching with the fabric is also crucial. For example, the aerogel mentioned above is fragile and can easily collapse under external force, so it is unsuitable for direct application in infrared stealth fabrics. Doping CNTs in silica aerogel can avoid the cracking or collapse of the delicate aerogel layer since the high elastic modulus property of CNTs, which makes aerogel a satisfactory thermal insulation layer [48].

1.3.4 Previous Research on Infrared Stealth Fabric

Metals are widely used in infrared stealth fabrics due to their high reflectivity and thus low emissivity. Jia et al. used magnetron sputtering to form a nanoscale copper film on aramid fabrics, and the infrared emissivity of the fabric could reach 0.1 [49]. Peng et al. coated a titanium dioxide/copper/titanium dioxide (TiO_2/Cu/TiO_2) sandwich structure on the surface of fabric by magnetron sputtering [50]. The bottom TiO_2 acts as a buffer layer on the surface of the fabric to improve the flatness of the fabric and improve the sputtering quality of the middle

copper layer, while the upper layer of TiO_2 plays a protective role. The infrared emissivity of the fabrics can reach 0.7. Because of the protective layer (upper TiO2 layer), it shows good washing fastness and moderate crocking fastness.

Metallic pigments have high reflectivity in the infrared range, but they are hard to apply to stealth technology directly due to their high glossiness [51]. Different approaches could be used to fix this weakness. Wang et al. modified aluminum pigments with reduced graphene oxide (rGO) to reduce the gloss of the pigment so that the paint can be better applied to stealth technology [52]. The visual gloss of the prepared coating can be suppressed by 58%, and visual light reflectivity was reduced by 23% with a slight increase of LWIR emissivity. After the paint was applied to the fabric, the infrared emissivity ranged from 0.6 to 0.8, depending on the ratio of rGO: Al. Instead of developing new types of coatings, Larciprete took a different approach. They produced fabrics with stainless steel fibers to prepare infrared stealth fabrics, and the MWIR emissivity of the fabricated fabrics was around 0.5 [53]. They found that the metal oxide formed after iron is exposed to oxygen will greatly increase the infrared emissivity of the fabric, so a protective film on the surface of stainless steel is very important.

Due to the existence of an energy band gap and low carrier concentration, intrinsic semiconductors do not have good infrared stealth performance. However, after doping, the carrier concentration increases, which increases optical conductivity and in turn the infrared reflectivity. Several studies have shown that the infrared emissivity of coated fabrics is strongly related to the doping level [54-56]. Mao et al coated Al, La-doped zinc oxide (ZnO:(Al, La)) nanoparticle coatings on fabrics to effectively reduce the infrared emissivity of fabrics [54]. They found that the infrared emissivity of the fabric decreased as the particle size of ZnO:(Al, La) decreased. By carefully adjusting the Al content, they found that when the Al content is 5%, the emissivity of the coated fabric is the lowest. Higher Al content increases the probability of infrared photons being scattered, so the emissivity slightly increases.

Some research attempts integrate low-emissivity materials with heat-insulating materials to achieve better stealth performance. Xu et al. hot-pressed CNT-doped aerogels (CNTAs) with two pieces of polyimide fabrics and then coated Al-doped zinc oxide (AZO) as a reflective layer on the fabricated sandwich-structured fabrics [48]. The infrared emissivity of the final

prepared fabric is less than 0.5. Due to its own porosity, aerogel has extremely low material density and low thermal conductivity, which can reach 0.013 W/(m·K) [57]. And the article pointed out that the addition of aerogel can significantly improve the flame retardancy of the fabric. The doped CNTs can avoid the cracking or collapse of the delicate aerogel layer due to their high elastic modulus. Wang et al. coated mesoporous carbon-aluminum doped zinc oxide (C-AZO) coatings on cotton fabrics to achieve the effect of infrared stealth [58]. High porosity of mesoporous carbon guarantees its thermal insulating property. They found that increasing the content of C-AZO can significantly reduce the emissivity of the fabric. When the content of C-AZO reaches 30 wt%, the LWIR emissivity does not change significantly due to particle aggregation and remains at about 0.8.

Gu et al. coated double-shell microcapsules (DSMs) of eicosane on the inner layer and polyaniline (PANI) on the outer layer of fabric [59]. Eicosane is a phase change material that can be used as a temperature control layer due to latent heat. At its transition temperature, absorbed heat will first be used in the phase change, so the temperature will be stay until the phase change is finished. The conductive polymer PANI has extended conjugated double bonds. The delocalized π-bond electrons are not bound by atoms and can move freely on the polymer chain, which provides its metallic properties, so it is used as the material of the reflective layer. Hollow glass microspheres (HGMs) are also a material commonly used in the field of infrared stealth due to their low thermal conductivity and wave absorbing ability. Since it does not have reflection capability, HGM is often combined with other high reflectivity materials to achieve the effect of dual-band stealth. Zhou et al. coated PANI-coated hollow glass microspheres (PANI/HGMs) doped with zinc oxide (ZnO) on Ag-deposited cellulose fabrics to prepare fabrics with both infrared and electromagnetic interference (EMI) stealth effects [60]. Among them, the silver layer mainly plays the function of reflecting infrared rays, and the HGMs with PANI coating can better absorb electromagnetic waves and provide temperature control effects. In addition to providing ideal thermal and chemical stability, ZnO nanoparticles also have good electromagnetic wave absorption capabilities.

The infrared emissivity of the outdoor environment is often not a fixed value and is strongly affected by factors such as temperature, solar intensity, and humidity. Therefore, the

stealth ability of the target with an unadaptable low emissivity fabric may be weakened when the environmental factors change. Therefore, it may be necessary to develop materials whose emissivity can change with the environment. Mao et al. used W-doped vanadium dioxide (VO_2) as a phase change material to prepare infrared stealth fabrics [61]. Due to the thermochromic effect, W-doped VO_2 can transform from a semiconductor state to a metallic state when the temperature exceeds the transition temperature, which greatly reduces the infrared emissivity. The article points out that the transition temperature decreases with increasing W doping. However, W doping will also reduce the phase transition ability of VO_2, so the emissivity difference before and after the phase transition decreases. Ergoktas et al. hot-pressed layers of multilayer graphene (front electrode), fabric (middle layer) and conductive fabric (back electrode) [62]. Ionic liquid electrolyte was added to the back electrode as a final step to prepare infrared stealth fabric with voltage-controlled emissivity. Under the influence of the voltage, the ions in the back electrode can intercalate the graphene layer and increase the carrier concentration in the graphene layer [63]. Due to the increased electron density, the infrared emission of the graphene layer drops drastically. Through experiments, the infrared emissivity of the fabric is adjustable in the range of 0.35 to 0.7. By replacing the conductive fabric with an electrode array with a control circuit, the emissivity of the fabric at different locations can also be controlled.

After decades of research and development, the performance of infrared stealth fabrics has been continuously improved. However, current stealth fabrics still have apparent deficiencies in the following aspects:

1. The emissivity of the fabric is still high. Due to the high surface roughness of fabric, most of the coatings that can exert good infrared stealth performance on a relatively flat substrate are greatly weakened on the fabric. For example, the LWIR emissivity of the C-AZO composites mentioned above [64] is around 0.4 when using an aluminum sheet as a substrate. However, the emissivity goes up to nearly 0.8 when the substrate is changed to fabric [58]. At present, the infrared stealth emissivity of most research is about 0.7 in the far infrared range, which cannot match the rapidly developing infrared detection technology. Therefore, it is very important to find coatings that can still have good stealth performance

on fabric substrates.

2. The process of preparing the stealth fabrics is relatively complicated, and the raw materials and preparation methods are difficult to be applied to the current fabric industry. Some papers used magnetron sputtering to coat a reflective layer on top of the fabric, which is not common or easy to be achieved in the textile industry [49], [50]. Others use materials that have no commercial suppliers, such as CNTA, and they need to be prepared in multiple steps from the raw materials. What's worse, a lot of the raw materials do not meet the current environmental and health requirements of the textile industry, which make industrialization even harder.
3. Most infrared stealth coatings will greatly reduce the original advantages of fabrics. Many coatings will cover the original color of the fabric after being coated on the fabric, and weaken the thermal, moisture, air permeability, and flexibility of the fabric. And because of the low infrared efficiency of coatings discussed in limitation 1, the coating thickness of many infrared stealth fabrics needs to reach hundreds of microns to meet the requirements of emissivity, which further weakens the original performance of the fabric. A thick coating will also greatly damage the good diffuse reflectance performance of the fabric.

1.4 Thesis Organization

Although not all of the specific problems of e-textiles and infrared stealth fabrics are the same, a shared common problem is the incompatibility of fabric functionality (such as electrical conductivity and stealthing performance) and wearing comfort. Reasons for this include the rough, porous surface of the fabric which prevents many materials from being compatible with it, fabric's low thermal tolerance, and electronic and stealthing materials not being optimized for things like vapor transmission and mechanical flexibility. Most of the current research on smart textiles only focus on the exploration and verification of new textile functions. This study addresses a need to test the materials and preparation methods of smart textiles to maximize the coexistence of performance and comfort. Chapter 2 will solve the problem of fabric wearability reduction caused by TPU film as the intermediate layer. The influence of different kinds of TPU films on the performance of e-textiles will be studied and discussed in detail. The influence

of different processing conditions on the performance of e-textiles will also be involved. Chapter 3 will propose AgNWs as a new material that can be used to prepare infrared stealth fabric to solve the problems of insufficient stealth performance and complicated preparation methods of infrared stealth fabrics. The stealth performance of the material and the degree of adaptation to the fabric are criteria for selecting this material. In order to further improve the performance of infrared stealth textiles, the latter part of this chapter will optimize material parameters, formulations and processing conditions. Chapter 4 will summarize the key findings of this study and discuss future optimization directions and methods for these two smart textiles.

TPU films are also used as the encapsulation layer of many smart textiles (i.e., they are not limited to e-textiles), and the development of infrared stealth fabrics is very similar to the preparation ideas of many other smart textiles (such as thermal management fabrics). Therefore, the results of this work are not limited to providing data for the research of two smart textiles but provide guidance for future research on similar smart textiles.

Chapter 2

Mitigating the Impact of Thermoplastic Polyurethane Films on the Wearability of Electronic Textiles

2.1 Introduction

As discussed in Chapter 1.2, the use of TPU film as an intermediary layer in e-textiles is common as it brings large improvements in the device performance and cost of e-textiles. However, at the same time, its mismatch with the modulus of the fabric and obstruction of the fabric's porosity reduces the comfort of human wearing. Therefore, it is crucial to optimize and adjust the TPU film and processing conditions so that e-textiles can better maintain the original advantages of the fabric, such as breathability and drape while at the same time have good electronic properties. To the best of my knowledge, there has yet to be research in this direction. In this chapter, I explore the influence of TPU type, its thickness, and the heat lamination parameters on the conductivity, rigidity, water vapor permeability (WVP), thermal permeance and stretchability of e-textiles. The results provide guidance for the selection of TPU films in the preparation of e-textiles.

A portion of this chapter has been published as: Tiancheng Xu and Irene A. Goldthorpe, "Mitigating the Impact of Thermoplastic Polyurethane Films on the Performance of Electronic Textiles [65]".

2.2 Materials and Methods

2.2.1 Materials

Nine types of TPU film (Single-layered: DS3412, DS8502, DS8613, UAF438, UAF472, UAF487; Double-layered: APF500, ST503, ST604), some types with multiple thicknesses, were purchased from three vendors (Tunsing Plastic Products Ltd., Bemis, and Adhesive Films Inc.). Double-layered TPU films contain both an adhesive layer and a printing layer with a higher

melting point. The textile used was a stretchable nylon spandex fabric (80% nylon, 20% spandex, FabricLA) appropriate for use in athletic wear.

2.2.2 Sample Fabrication Procedure

Samples for flexibility, water permeance and thermal tests were fabricated by laminating TPU film onto the fabric using a heat press (Flex Heat Transfer Vinyl Ltd.). Fabric without TPU was also measured for comparison. To determine the impact of TPU and lamination conditions on conductivity and stretchability, conductive silver ink CI-1036 (containing silver microflakes) purchased from EMS Inc. was screen-printed by hand onto the TPU films before their lamination (Figure 2-1(a)). Stainless steel screens from UTZ technologies were used (80 mesh count, 0.002-inch mesh opening, 0.0008-inch emulsion thickness, 15° mesh angle). 1.5 x 1.5 cm and 1.5 x 2 cm printed ink patterns were used in the conductivity and stretchability measurements, respectively. The ink was cured in a low vacuum oven at 100 °C for 10 minutes after printing. Subsequently, the TPU-ink was laminated onto the nylon spandex fabric at 120 °C for 20 s unless stated otherwise. As a control, ink was also directly printed on fabric without TPU, also cured at 100 °C for 10 minutes (Figure 2-1(b)).

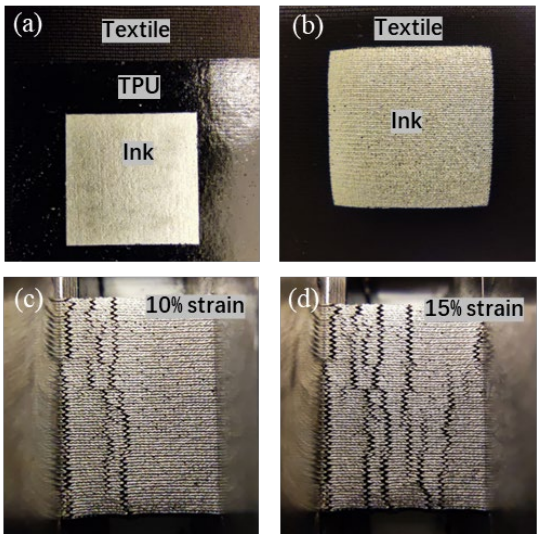

Figure 2-1: (a) Conductive ink on TPU film laminated on fabric. (b) Sample fabricated by directly printing conductive ink on the fabric. Obvious cracks of the directly printed sample with (c) 10% and (d)15% strain. The printed ink size is 1.5 x 1.5 cm.

2.2.3 Characterization Methods

Flexibility tests to measure stiffness or drape were conducted based on the BS-3356 standard [66] using a cantilever tester (XHF-42A Fabric Stiffness Tester). The flexural rigidity of the sample was calculated from the mean bending length and the mass per unit area of the sample.

WVP tests measure the samples' breathability. The WVP measurements were conducted based on the Dry Cup method in ASTM D-1653 [67]. The textile-TPU composite covered the top opening of a 10 cm diameter petri dish with desiccant. The samples were put into a chamber with a relative humidity of 99% and temperature of 21 °C, and the petri dish weight changes were recorded daily. The WVP is derived from the average weight change, sample surface area, and ambient humidity and temperature.

The thermal transfer of the sample depends not only on its thermal conductivity but also on the cooling effect brought by the transmission of water vapor (i.e., sweat). In this experiment, the textile-TPU composite covered the 8 cm diameter top opening of a beaker filled 70% full of hot water. The temperature difference between the two sides of the sample was measured and recorded by temperature sensors. The water temperature was kept at 90 °C using a hot plate to make sure water vapor was generated at a constant and mild speed. The average stabilized temperature difference after 15 minutes was used to assess the fabric's thermal performance. A higher temperature difference indicates that the thermal permeance of the fabric is worse, meaning that the textile-TPU traps heat which typically reduces the comfort of the human body. This is particularly important for e-textile device applications which generate heat as a by-product, such as medical light therapy.

The sheet resistance of the printed ink after curing and lamination was measured with a four-point probe (Ossila Ltd.). Strain cycling tests were performed to assess stretchability. Unlike traditional electronics, many e-textiles are regularly subjected to stretching in everyday use. Electronic performance should change as minimally as possible after repeated strain. 50 cycles of 30% strain at a speed of 5 mm/s were applied using a linear stage (X-LHM150A, Zaber Technologies) and a digital multimeter (SDM3045X, Siglent Technologies) simultaneously measured resistance. The resistance at 300 ms after each stretching and relaxing step was recorded

to gain a more stable multimeter readout. TPU surface roughness was measured using a Bruker Icon atomic force microscope.

2.3 Effect of TPU Film Thickness

To investigate the effect of TPU film thickness on e-textile performance, TPU of the same type (DS8502) but different thicknesses were used. Figure 2-2 shows the effect of TPU thicknesses on the sample's flexibility, breathability, and thermal performance. It can be seen in Figure 2-2(a) that compared to pure fabric (blue triangle), laminated TPU on fabric significantly increases the flexural rigidity of the sample (i.e., increases stiffness). In Figure 2-2(b), we see that TPU on the surface of the fabric hinders the transmission of water vapor, leading to lower WVP. Thirdly, as per Figure 2-2(c), TPU on fabric increases the temperature difference between the front and back of the sample, meaning that TPU hinders thermal transport. This is both because the TPU prevents high-temperature water vapor from being quickly transported to the other side of the fabric to assist temperature exchange and because the additional layer causes slower thermal conduction. In all cases, increasing the thickness of the TPU film will further reduce the flexibility, breathability, and thermal permeance of e-textiles. The thickness of the TPU film has an almost linear relationship with the flexural rigidity, WVP, and temperature difference, and no saturation trend is found.

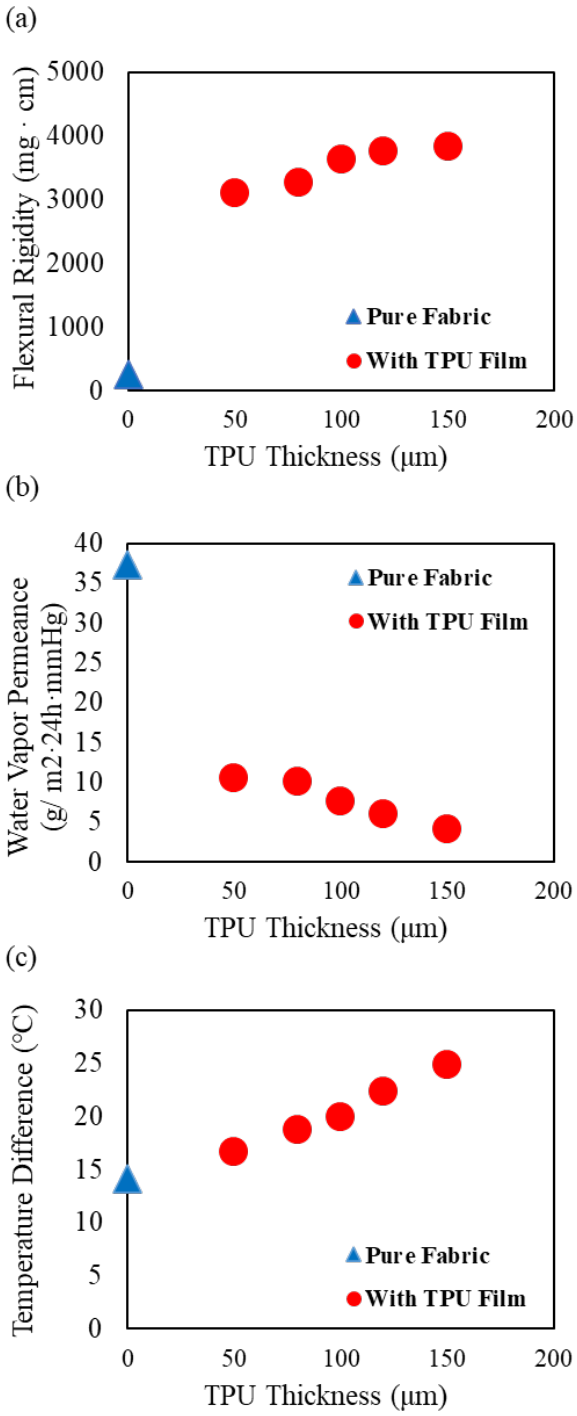

Figure 2-2: Impact of different thicknesses of TPU on: (a) flexibility, (b) breathability, and (c) thermal permeance. Blue triangles correspond to fabric without TPU, and red circles correspond to TPU (DS8502) with different thicknesses laminated on the fabric.

Figure 2-3 shows the effect of TPU films with different thicknesses on the conductivity and stretchability of the sample. It can be seen from Figure 2-3(a) that as the thickness of the TPU film increases, the resistance of the prepared samples improves. This is because, during the lamination process, the TPU softens and gets pushed into the pores of the fabric, causing its

surface to deform. This in turn deforms the printed layer of conductive silver ink, increasing its resistance value. From Figure 2-4, it is observed that as the TPU thickness increases, the ink surface is more even with less apparent fabric texture. Thicker TPU film can play a buffer role more effectively in lamination and relieve the deformation of conductive silver ink.

Figure 2-3(b) plots the change in resistance of TPU-fabric samples when subjected to 30% strain for 50 cycles. The resistance increases much less as TPU thickness increases, showing that the use of thicker TPU leads to better stretchability performance. This is firstly because, as just discussed, the silver conductive layer is less damaged during the lamination process when thicker TPU is employed. Secondly, the fabric does not elongate uniformly when stretched, and thicker TPU leads to a more even strain along the printed conductive layer. Less cracking in the ink layer was observed when thicker TPU film was used. However, due to the viscoelasticity of the TPU film, samples undergo some plastic deformation during stretching. Figure 2-3(c) shows the residual (i.e., remaining) strain of TPU films with different thicknesses after 50 stretching cycles. Increasing the thickness of the TPU film will make the mechanical properties of the prepared e-textiles more inclined to the TPU film, and the residual strain will increase. Choosing a more elastic TPU film in e-textiles would be preferable.

Figure 2-3 excludes the case where conductive ink is printed directly on fabric without TPU (Figure 2-1(b)). The sample was fragile, having a weak connection between the ink and the fabric. As per Figure 2-1(c) and (d), the sample could not handle small external forces, sustaining severe cracking and an electrical open circuit at small strains.

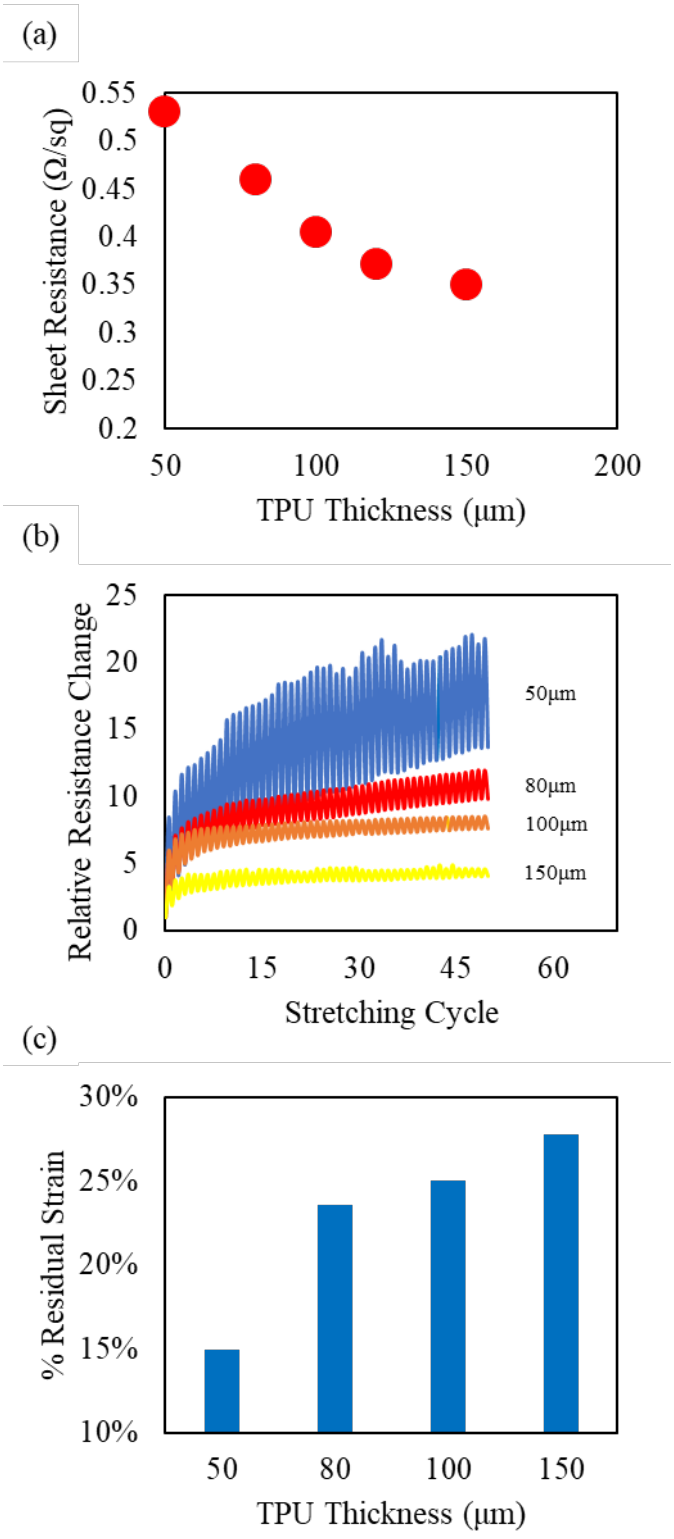

Figure 2-3: Impact of different thicknesses of TPU film (DS8502) on the sample's (a) conductivity and (b) stretchability. (c) The residual strain of the samples with different TPU thicknesses after 50 cycles of 30% strain.

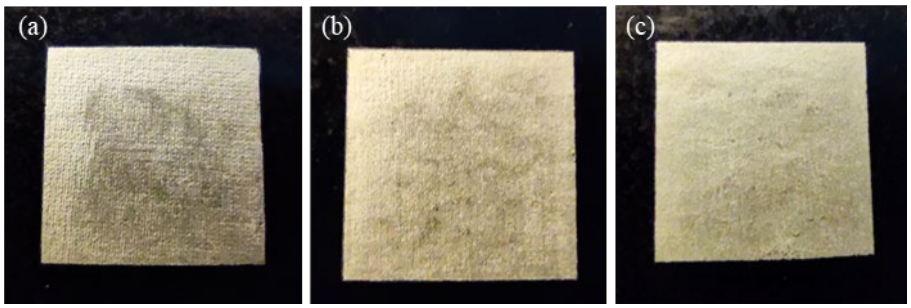

Figure 2-4: The surface morphology of ink printed on TPU films then laminated, with TPU thicknesses of (a) 50 µm, (b) 100 µm, and (c) 150 µm. The ink layer is 1.5 x 1.5 cm.

2.4 Effect of TPU Type

TPU films of different types but the same thickness were tested next. Figure 2-5 displays the dependence of flexibility, breathability, and thermal performance on TPU density. In Figure 2-5(a), we see that denser TPU types are more rigid. This is because denser TPU film has higher crystallinity which implies more tightly packed molecular chains in the polymer. The rigidity of these crystalline segments is greater due to the close arrangement of molecular chains. TPU film with a lower density leads to better flexibility of the e-textile. In Figure 2-5(b), it can be seen that the WVP of the sample decreases with increased TPU density since it is more difficult for water to transport through the tightly packed crystalline hard segments.

Because heat is transferred across a textile by more than one mechanism, its dependence on density is not as straightforward. On one hand, high-temperature water vapor (e.g., sweat) can better permeate lower-density TPU. On the other hand, lower-density TPU films tend to contain more randomly arranged amorphous molecular chains. This increases the probability of phonon scattering, reducing their mean free path, which in turn lowers thermal conductivity [68]. These competing effects result in the temperature difference plotted in Figure 2-5(c) to first decrease and then increase with increasing TPU film density.

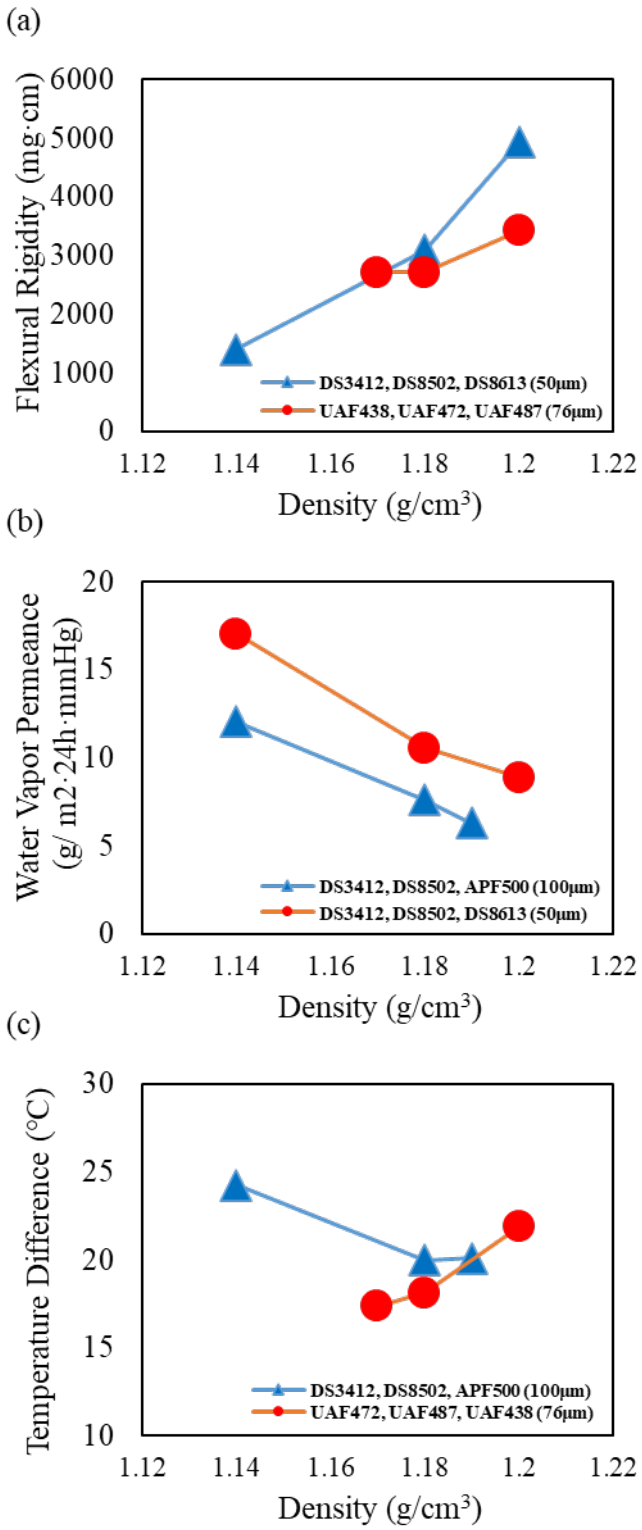

Figure 2-5: Impact of TPU density on the sample's (a) flexibility, (b) breathability and (c) thermal permeance.

We found that the density of the TPU film has no noticeable effect on electronic performance. However, a large effect is seen when using single versus double-layered TPU film. Figure 2-6 describes the effect of single-layered and double-layered TPU film on the conductivity and

stretchability of e-textiles. In Figure 2-6(a), the resistance values of ink upon double-layered TPU film are lower than those upon single-layer TPU films that are the same thickness or thicker. Due to the higher melting point of the upper printing layer, it better resists pressure deformation during heat lamination, and thus the structure of the printed conductive ink remains better intact. What is more, the better mechanical isolation between the TPU top surface and the fabric means that the ink is more likely to be stretched evenly when subjected to stretching. Therefore, the stretchability of samples prepared using bilayer TPU film is far superior (Figure 2-6(b)).

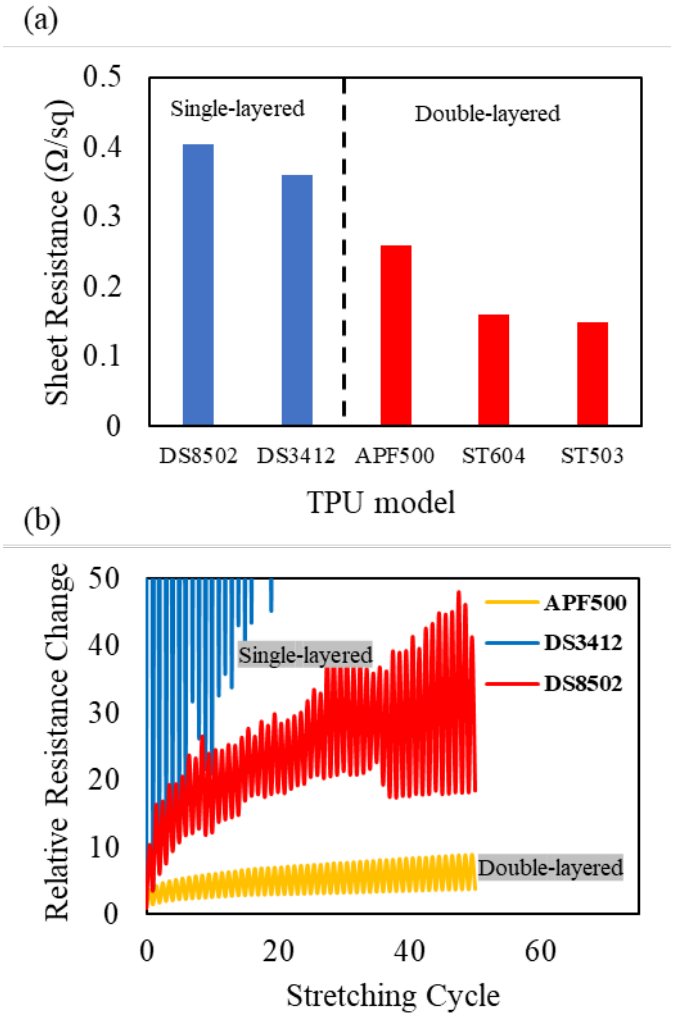

Figure 2-6: Impact of single versus double layered TPU film on the sample's (a) resistance and (b) stretchability.

Substrate roughness is an important factor when considering printing quality in many applications [69]. However, the arithmetic average roughness (R_a) of the various TPU films used here is mostly less than 30 nm, whereas the thickness of the conductive layer is greater

than 25 μm. Therefore, when tested, it was found that the surface roughness of the TPU film did not strongly affect the resistance value of the printed ink in this study.

2.5 Effect of Processing Conditions

In addition to choosing different TPU films and thicknesses, optimizing the lamination conditions can also significantly improve e-textile performance.

There are two heat treatments in the preparation process, namely, the heat curing of the conductive silver ink and the heat lamination of the TPU-silver ink and the fabric. During curing, the degree of fusion between the silver flakes will be improved, the junction resistance between the flakes will be reduced, and the conductive silver ink will form a robust conductive layer. Therefore, increasing the curing temperature and/or time will greatly improve the conductivity and stretchability of the sample. Nevertheless, it is worth noting that the softening point of most TPU films is between 80 and 120℃. When dealing with circuits with higher resolution, it is necessary to recognize that the curing temperature should not be higher than the softening point of the TPU film to reduce the risk of a short-circuit. Concerning double-layered TPU films, the printing layer and the adhesive layer have different melting points. If the curing temperature is between the two melting points, the melting and expansion of the adhesive layer are likely to cause sample bending (Figure 2-7). The curved TPU-silver composite means that the silver layer will be subject to greater deformation when it is laminated with a flat fabric, resulting in a significant drop in electric properties. Therefore, it is vital to control the curing temperature reasonably or immobilize the sample when processing double-layer TPU film.

Figure 2-7: The curvature of APF-500 when the curing temperature is 100 °C. The melting points of the adhesive layer and printing layer are around 90 °C and 150 °C, respectively.

Regarding lamination, Figure 2-8(a) shows the flexural rigidity of the TPU-fabric composite when different lamination conditions are applied compared to using the standard parameters (120 °C, 20 s, 32 mm). Higher temperature, longer time, and larger pressure during lamination all decrease the mechanical flexibility (increases stiffness) of the samples as it forms a more compact fabric-TPU composite. The mildest lamination conditions, i.e., lowest time, temperature, and pressure result in the least increase in rigidity. It was found that the breathability and thermal performance of e-textiles have no obvious relations with the lamination conditions.

Figure 2-8(b) describes the change in the resistance value of the silver conductive layer before and after lamination when different lamination conditions are used. At lower lamination times and temperatures, the resistance increases because of the deformation of the conductive ink layer. Although deformation still occurs at higher lamination temperatures and times, the resistivity is improved at these conditions due to the contribution of improved ink curing. Because of the low thermal tolerance of TPU, the ink curing temperature was limited to 100 °C, below the optimal curing temperature of printable conductive ink. Higher lamination times and temperatures can sufficiently further evaporate the solvent in the conductive silver ink and enhance silver flake fusion that was incomplete from the low-temperature cure. Lastly, while relatively high pressure can fasten the heat transferring from the hot plate to the sample, excessive pressure can cause the underlying rough fabric to press against the conductive ink layer, causing this layer to deform. Therefore, moderate pressure is beneficial to improve the conductivity of e-textiles.

Figure 2-8(c) depicts the variation in the stretchability of the samples under different laminating conditions. It can be seen that increasing the time, temperature, and pressure all increase the stretchability performance of the prepared sample. This is first because lamination improves flake fusion, as discussed above, and it is known that better welded nanoparticle junctions increase ink flexibility [70]. Secondly, lamination can improve the degree of fusion between the TPU film and the silver ink layer. The improved adhesion of the silver ink with the substrate can elicit more uniform stretching, thereby avoiding apparent cracks. The lamination effect also helps explain a previous result in the literature that ink on TPU subsequently laminated to fabric maintains better conductivity after strain cycling than ink on TPU alone [41].

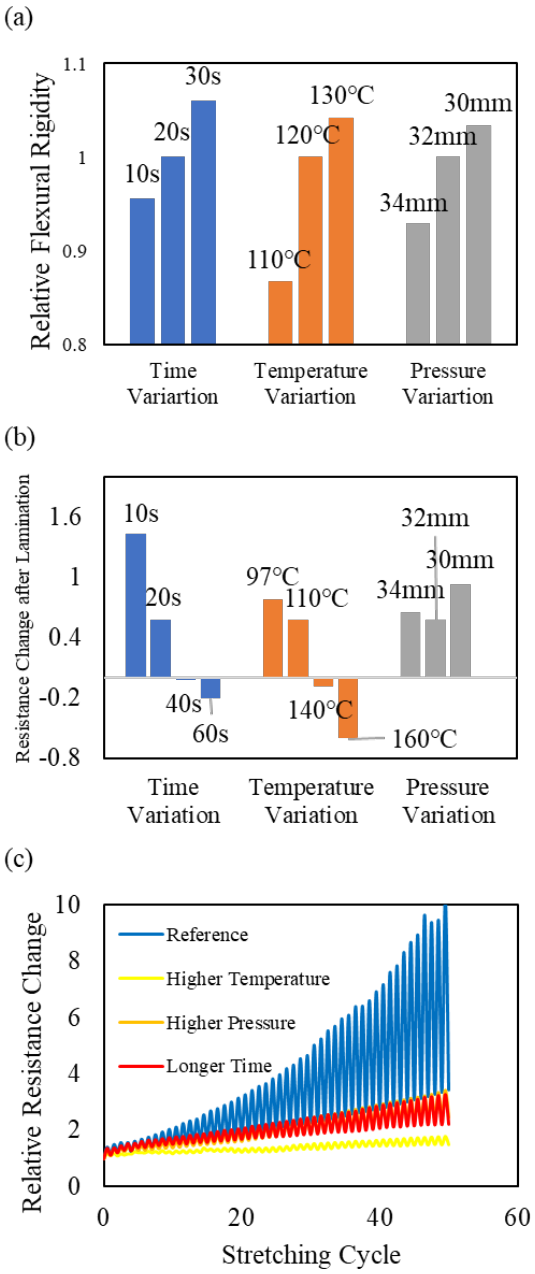

Figure 2-8: Impact of lamination time, temperature and pressure on the sample's (a) flexibility, (b) conductivity, and (c) stretchability. APF-500 was used in these experiments. Pressure is evaluated through the distance between the upper plate and the pressure knob, with lower values corresponding to higher pressure. Experiments were conducted by changing one variable at a time. The standard lamination parameters (120 °C, 20 s, 32 mm) are used in (a) as the reference condition. The reference condition in (b) and (c) are 110 °C, 20 s, 32 mm and 120 °C, 30 s, 34 mm, respectively.

2.6 Conclusion

It was found that the selection of TPU and its lamination conditions can make a substantial impact on the performance of an e-textile. TPU thickness needs to be considered in light of the needs of the application. On one hand, thicker TPU has a positive effect on the electrical conductivity and stretchability of the e-textile, but the drape, breathability, and thermal permeance of the textile are sacrificed. Less dense TPU types are preferred as they have improved breathability and thermal transport. Double-layered TPU film was found to more effectively avoid the influence of the fabric on the conductive silver ink, thereby improving the conductivity and stretchability of the e-textile. Higher curing temperature and time can fuse the silver flakes together and improve the electronic performance of the e-textiles, but melting and curling of TPU film will occur when the temperature is too high. Lastly, increasing the temperature and time of lamination can effectively improve electrical properties, but the e-textile becomes more rigid. For future work, other strategies to minimize the impact of the TPU on the textile can be explored, such as cutting holes in the TPU layer between circuitries.

Chapter 3

Selection and Performance Optimization of Materials for Infrared Stealth Fabrics

As was seen in the literature review in 1.3.4, current infrared stealth coatings have the deficiencies of high infrared emissivity, complicated raw materials and preparation processes, and impairing the original nature of the fabric. In this chapter, a new coating material for infrared stealth fabrics will be presented and optimized. TPU film is not used here, as will later be explained. Similar to the previous chapter, the goal is to improve the functionality of the fabric (reduce emissivity in this case) while retaining the original properties of the fabric. In section 3.1, the reason of choosing AgNWs as a better material for infrared stealth coating will be discussed. The optimization of the parameters of AgNWs and how to further exploit the advantages of AgNWs through resins and adjustment of curing temperature will be discussed in section 3.2.

The research was done in cooperation with Alchemy Company. Due to confidentiality regulations, the specific optimization of the AgNW solution formulation will not be presented in this chapter.

3.1 Material Selection

Thermal insulation materials and low emissivity materials are the two mainstream choices for infrared stealth fabric coating materials. Thermal insulation materials will greatly hinder the original thermal performance of fabrics and reduce the comfort of clothing when wearing. Therefore, low emissivity materials have more advantages in ensuring the original performance of fabrics and become the material choice for this research. Considering the infrared stealth efficiency of the coating material, the degree of matching with the fabric substrate, and the guarantee of the original fabric performance, AgNWs are considered to be a very suitable material for infrared stealth fabric coatings.

AgNWs refer to a one-dimensional silver metal nanomaterial with a cylindrical shape, whose length is in the micrometer scale and the diameter is in the nanometer scale. Its ultra-long aspect ratio and excellent conductivity make it play an important role in many research fields, such as wearable devices, transparent electrodes, and flexible displays [71], [72]. One of the advantages of AgNWs as an infrared stealth coating is related to their unique optical properties. In subsection 3.1.1, relevant background knowledge and models used for optical simulations of AgNWs are introduced and discussed. In subsection 3.1.2, the merits of using AgNWs will be discussed.

3.1.1 Simulation of Optical Properties of AgNWs

3.1.1.1 Fresnel equation

When a beam of light enters a medium from another medium and the optical impedance of the two mediums is not the same, part of the light will be reflected to ensure the continuity of the electromagnetic field on the interface. Assuming that light is incident on the surface of an object from a vacuum (air), a special case of the Fresnel equation (Formula 5) can be deduced through the continuity equation on the interface [73]:

$$R = \frac{(n-1)^2+k^2}{(n+1)^2+k^2} \tag{5}$$

where R is the reflectivity of light, n is the refractive index of the object, and k is the extinction coefficient of the object. n and k are the real part and imaginary part of the complex refractive index $\tilde{n}$. $\tilde{n}$ is defined as $n + ik$ instead of $n - ik$ in this research.

3.1.1.2 Lorentz-Drude model

From the wave perspective, when an electromagnetic wave enters an object, the free electrons on the surface of the object vibrate under the action of the wave, forming secondary waves. These electron-generated waves add up and form two secondary waves that emit in different directions. The secondary wave in the same direction as the incident wave (forward wave) suppresses the incident wave. The suppressing degree depends on the number of electrons that

can freely move. The secondary wave in the opposite direction (backward wave) to the incident wave forms a reflected wave.

Due to the large number of free electrons contained in metals, the phase difference between the field generated by electron vibration in metal and the incident field is close to 180°. Therefore, the forward wave cancels out the incident light, and the backward wave forms the reflected light, which explains metal's high light reflectivity. The response of electrons to electromagnetic waves in ideal metals, that is, the dielectric function, can be represented by the Drude model. By solving the motion of free particles under the action of electromagnetic waves, the dielectric function can be expressed by Formula 6 [74].

$$\epsilon(\omega) = 1 - \frac{\omega_p^2}{\omega(\omega + i\Gamma_0)} \tag{6}$$

where ε is the dielectric function, ω is the frequency of the electromagnetic wave, ω_p is the plasma frequency of the material, and Γ_0 is the damping rate of the material. ϵ is always a complex number and is defined as $\epsilon_{r1} + i\epsilon_{r2}$ in this research.

By assuming that there is no magnetic response of the material, the complex refractive index $\tilde{n}$ can be derived from the dielectric function easily through Formula 7 [74]:

$$\tilde{n}^2 = \epsilon \tag{7.1}$$

$$n = \frac{1}{\sqrt{2}}[({\epsilon_{r1}}^2 + {\epsilon_{r2}}^2)^{1/2} + \epsilon_{r1}]^{1/2} \tag{7.2}$$

$$k = \frac{1}{\sqrt{2}}[({\epsilon_{r1}}^2 + {\epsilon_{r2}}^2)^{1/2} - \epsilon_{r1}]^{1/2} \tag{7.3}$$

where ε_{r1} is the real part of the dielectric function and ε_{r2} is the imaginary part of the dielectric function. n and k are the refractive index and extinction coefficient, respectively. The reflectance can in turn be solved by Formula 5. Figure 3-1 simulates the reflection of light by an object in the Drude model when gamma is set as 0.1, and the plasma frequency is set as 6. Plasma frequency represents the maximum frequency at which the metal electrons can participate in the response (vibration). When the light frequency is greater than this value, the metal loses its reflectivity and becomes transparent to light. Due to the existence of a mild damping rate value to simulate electron collision, a non-unity reflection value before plasma

frequency and a relatively smooth transition after reaching plasma frequency is shown in the figure.

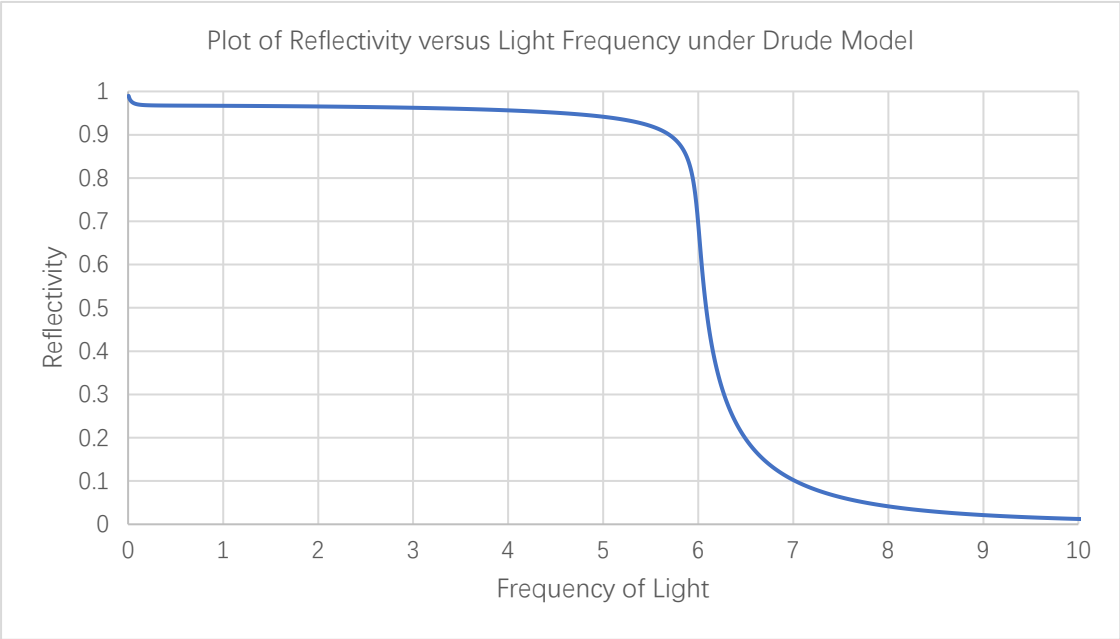

Figure 3-1: Simulation of an object's reflectivity under the Drude model. The plasma frequency is set as 6 and the damping rate is 0.1. MATLAB 2022a was used as the simulation tool.

In addition to free electrons, there are many bounded electrons in real metals. The response of these electrons to electromagnetic waves is similar to that of dielectrics, which can be expressed by the Lorentz model (Formula 8) [74]:

$$\epsilon(\omega) = \frac{\omega_p^2}{\left(\omega_j^2 - \omega^2\right) - i\omega\Gamma_0} \tag{8}$$

where ε is the dielectric function, ω is the frequency of the electromagnetic wave, ω_p is the plasma frequency of the material, ω_j is the resonant frequency of the material, and Γ_0 is the damping rate of the material. It can be seen that the difference between Formula 6 and Formula 8 is only the resonant frequency (ω_j). This parameter represents a bonding strength between the electrons and nucleus. When the frequency of light reaches or is greater than the resonant frequency, the response of electrons to the wave increases, and the reflectivity of the object rises. By adding the additional ω_j=2 parameter to the simulation, Figure 3-2 shows the reflection of light by objects in the Lorentz model. Combining Formulas 6 and 8, the well-known Lorentz-Drude (L-D) model can be obtained to represent the reflection of light by metals [74].

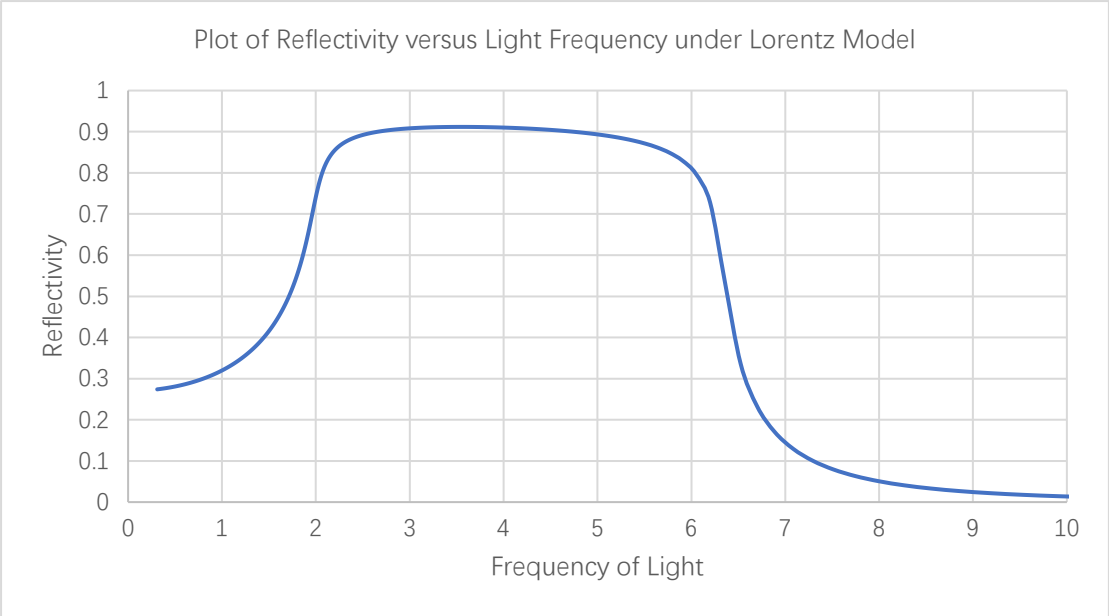

Figure 3-2: Simulation of an object's reflectivity under the Lorentz model. The plasma frequency is set as 6, the resonant frequency is 2, and the damping rate is 0.1.

3.1.1.3 Optical simulation of AgNWs

The AgNWs which are coated on fabrics in this work exist in a randomly-oriented mesh (Figure 3-3). Complex optical phenomena will occur when light is incident on such randomly distributed two-dimensional AgNW arrays, and Formula 5 cannot effectively solve the problem in this case. I first adopted the following simulation method. I established a random distribution of AgNW arrays in Ansys Lumerical 2020 and set the complex refractive index of silver (L-D model), the wavelength range of incident light, and the scale of the smallest simulation unit. Then the Finite-Difference Time-Domain (FDTD) method was applied to directly solve the reflection and transmittance parameters of the silver array for light. This method does not require physical approximation. However, due to the small diameter of AgNWs, to ensure the accuracy of the simulation, the smallest simulation unit is often about 5 nm. This caused the simulation time and memory required to explode acutely. An alternate method is to regard the nanowire-host material as a layer of homogeneous material, then calculate the effective dielectric function of the material through Maxwell-Garnett Effective Medium theory and bring the calculated optical parameters into the simulation software. A third method is to treat the randomly distributed AgNWs as a vertically intersecting metal mesh, which has a periodic

structure. These latter two methods can greatly shorten the time required for FDTD simulation, and they were both used in this chapter depending on the specific problem.

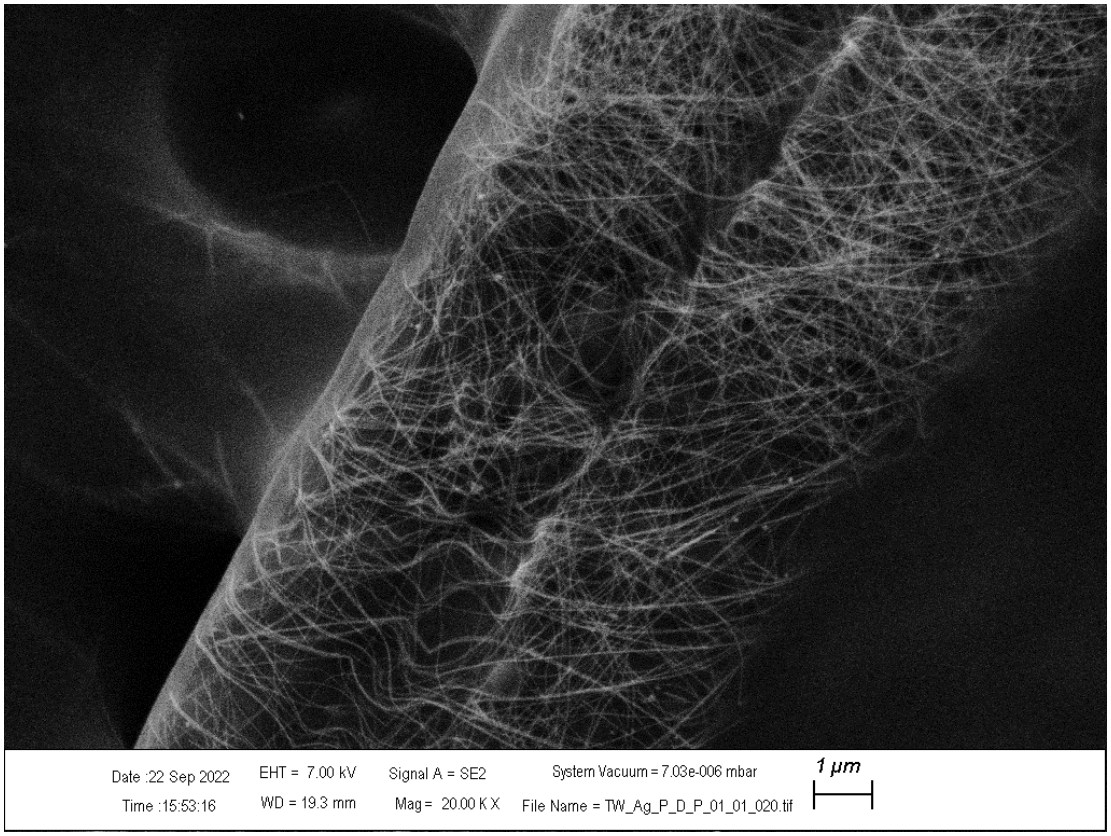

Figure 3-3: SEM image of AgNWs coated around the surface of a fiber. The diameter of the AgNWs is 30 nm.

3.1.2 AgNW Merits

The good reflectivity provided by metal is the first advantage of AgNWs in infrared stealth technology. Although the free electrons in doped semiconductors and conductive polymers also have reflectivity to infrared rays, the free electron density is still orders of magnitude lower compared to that of metals. Therefore, the amount of metallic coating required to achieve the stealth requirement is less and will thus have less impact on the other desirable properties of fabric.

I used the L-D model to calculate the dielectric function of bulk silver as a function of wavelength with MATLAB. Silver plasma frequency, resonant frequency, damping rate, and other parameters are extracted from the literature [74]. After substituting the dielectric function into Formula 7, the complex refractive index of silver can be obtained. Finally, through Formula

5, the reflectivity of silver to light with a wavelength range between 100 nm and 12 μm was obtained (Figure 3-4). It can be seen from Figure 3-4(a) that silver has a very high reflectivity (close to 1) to infrared light, which is very suitable as an infrared stealth material. In contrast, conducting polymers and doped semiconductors usually have a reflectivity of about 0.7 in the infrared region. In Figure 3-4(b), the response of free electrons to electromagnetic waves is shown for the wavelength range of 100 to 900 nm. The reflectivity in the ultraviolet part indicates the response of bounded electrons to electromagnetic waves, and two peaks are shown here, indicating different bonding strengths between bounded electrons and the nucleus.

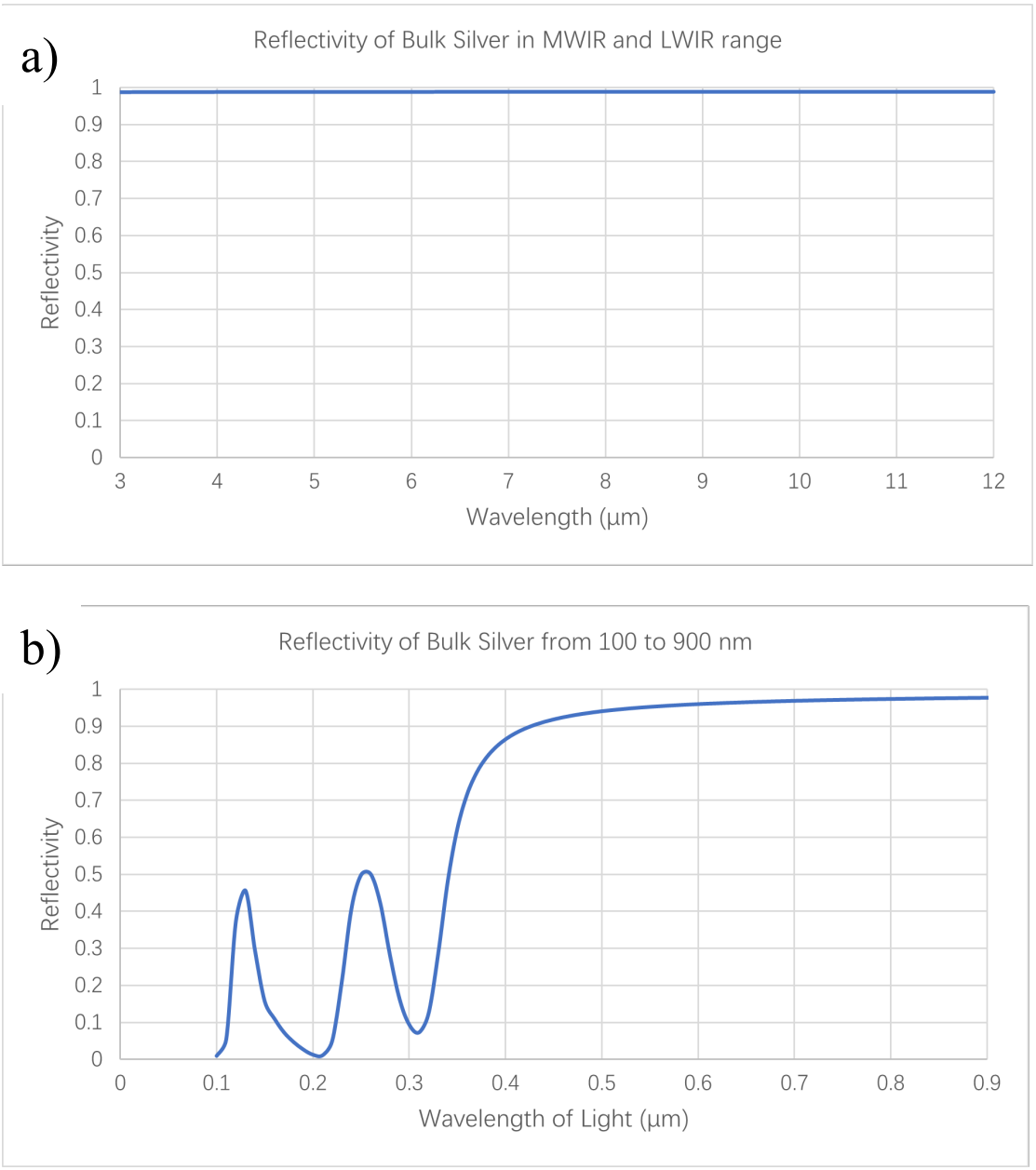

Figure 3-4: Simulation of bulk silver's reflectivity under the Lorentz-Drude model. The simulation wavelength range is from 3 to 12 μm (a) and 0.1 to 0.9 μm (b).

A silver film can be coated on the surface of fabric using magnetron sputtering, but this technique is expensive, difficult to scale to large areas, and not generally used in the textile industry. The silver film also cracks upon the repeated bending and stretching that is incurred in clothing, as seen in Chapter 2. Depositing silver in the form of a nanostructure, namely microflakes, nanowires, or nanoparticles (corresponding to two-dimensional, one-dimensional, and zero-dimensional materials, respectively), allows for pad coating, which is commonly used in the textile industry. The coating can occur in the atmosphere using a high-throughput roll-

to-roll method. Coatings consisting of silver nanostructures can also be very mechanically flexible [70]. The aforementioned silver nanostructures can all be synthesized in large batches in solution and are all commercially available to purchase. Silver nanostructures are already used in textile products, such as silver nanoparticles used in socks for their antimicrobial properties. I consider the different types of nanosilver next.

The first disadvantage of silver microflakes is their high gloss, which makes them unsuitable for stealth applications. In fact, the original purpose of many silver flakes is to increase the gloss of coatings and give objects a shiny appearance. The second disadvantage of silver flakes is their match degree with the fabric substrate. It can be seen from Figure 3-3 that the AgNWs can form a conformal layer of uniform network structure on the surface of a fiber. However, the diameter of silver flakes is relatively large (about 5 μm), which cannot make close contact with the fabric fibers, so it is difficult to spread evenly on the fibers after coating. AgNWs are nanometer-sized in two dimensions, which gives them high flexibility and stretchability to match the curved profile of the fiber [75]. The use of smaller diameter silver flakes (<1μm) may be a solution [76], but there are currently no similar products on the market. In comparison, AgNW with different diameters can be easily found in the market. Increasing the thickness of the layer to achieve a more uniform spread will hinder the original performance of the fabric. Also, the aforenoted shiny property of silver flakes will become more severe in this case and ruin the good diffuse reflection properties of the fabric.

The sizes of the silver nanoparticles are nanoscale in all three dimensions so that they can be better dispersed on the surface of the fabric fiber. But its infrared stealth efficiency is not as good as that of AgNWs due to the size effect [77]. When the size of the material is smaller than the mean free path of the electrons, the electrons collide at the metal grain boundaries. The mean free path of electrons in silver is about 53 nm [78]. In other words, electrons in silver nanomaterials smaller than this size are no longer "free". These collisions lead to increased energy losses (increased damping rate Γ), thereby lowering reflectivity. Instead of reflection, the energy of the light will be transmitted to the metal grain through collisions. Figure 3-5 shows the reflectivity and absorptivity of bulk silver in the range of 1-5 μm if the damping rate

is increased by 100%, and it can be seen that the reflectivity decreases and absorptivity increases.

From the above discussion, AgNWs have advantages over other forms of nanosilver for use as a fabric infrared stealth material.

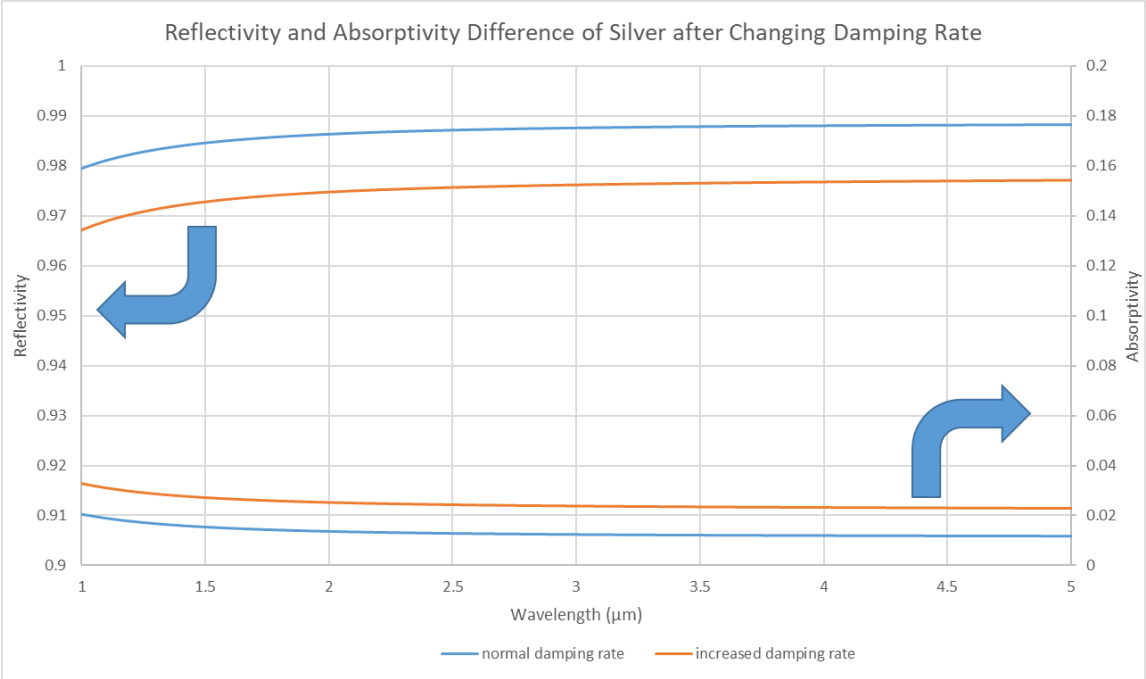

Figure 3-5: Reflectivity and absorptivity difference of bulk silver in the infrared range after doubling the damping rate.

Many articles point out the potential of AgNWs in infrared signature reduction. For example, Larciprete et al. studied the infrared properties of randomly oriented AgNW meshes on glass substrates and showed through both simulations and experiments that AgNWs can effectively block the transmission of infrared rays [79]. However, there are currently no research articles on the use of AgNWs as infrared stealth fabric coatings. Some devices that have similar working principles as infrared stealth fabrics, like personal thermal management devices and energy-saving windows, utilize AgNWs as their functional materials and will be briefly reviewed below.

Personal thermal management devices are wearable devices that reduce body heat loss and help maintain body temperature. Researchers often rely on the increasing infrared reflectivity of clothing to reflect infrared radiation back to the human body. Therefore, the high infrared reflectivity of AgNWs makes them suitable for this device. For example, Hsu et al. dip coated

AgNWs on fabrics to prepare thermal management clothing with good thermal insulation properties. When the mass loading of AgNWs is about 0.6 mg/cm^2, the infrared reflectivity of clothing is about 40% [80]. Choe et al. also mentioned that because the PVP on the surface of AgNWs is hydrophilic, only spraying AgNWs on one side of the hydrophobic fabric can prepare asymmetric hydrophilic fabrics, which can help sweat transportation and maintain body temperature better [81]. One difference between thermal management clothing and infrared stealth fabrics is that thermal management clothing can not only passively reduce heat loss but also actively heat up to cope with extreme temperatures. The Joule heat generated by a AgNW conductive matrix can meet this requirement. Hsu et al. mentioned in the article that AgNW network has a lower resistance than a CNT network, so the required voltage is lower when the same temperature is raised [80].

External heat radiation of buildings accounts for a large part of energy loss, so the working principle of energy-saving windows is to use their high infrared reflectivity to reflect the heat radiation of buildings. In fact, another name for energy-saving windows is low-emissivity windows. AgNWs have high infrared reflectivity, and their visible light transmittance can be adjusted by mass loading, so they are very suitable as coating materials for energy-saving windows. Lin et al. sprayed AgNWs/polyvinyl butyral (PVB) on windows to prepare energy-saving windows [82]. The reflectance of the prepared sample in the MWIR range reached about 70%, and the transmittance in the visible range was maintained at about 83%. The main application field of infrared stealth fabric is military. The high visible light transmittance of AgNW coatings can ensure that the coating will not cover the fabric's original camouflage patterns, which is another advantage of using AgNWs.

3.2 Parameters Determination and Subsequent Optimization

3.2.1 Silver Nanowire Size Determination

Nanowires of various diameters and lengths are commercially available, and the size selection of AgNWs is important as it affects the stealth fabric properties. Due to the relatively high cost of AgNWs, it is necessary to choose AgNWs with the highest reflectivity. Reflectivity is a

stronger function of radius than diameter. Under the same mass, a network with thinner nanowires has a higher number of wires in it, but a network formed by AgNWs with larger diameters is thicker. It is not obvious which one would lead to higher reflectivity, so the following simulation was built.

I used the L-D model and Maxwell-Garnett effective medium theory to calculate the effective dielectric function and complex refractive index of AgNWs with the same mass but different diameters. The size effect in the diameter direction of AgNWs was also taken into account. Formula 9 represents the effective dielectric function of the AgNWs randomly distributed on a plane [79]:

$$\varepsilon_{plane} = \varepsilon_e + \frac{f}{2}\varepsilon_e(\varepsilon_i - \varepsilon_e)\frac{\frac{1}{\varepsilon_e}+\frac{1}{\varepsilon_e+(\varepsilon_i-\varepsilon_e)/2}}{1-\frac{f}{4}\frac{(\varepsilon_i-\varepsilon_e)}{\varepsilon_e+(\varepsilon_i-\varepsilon_e)/2}} \quad (9)$$

where ε_{plane} is the effective dielectric function along the plane, ε_i is the dielectric function of AgNWs obtained by the L-D model, ε_e is the dielectric function of the host material, and f is the fill factor which means the ratio of the cross-sectional area of the AgNW to the total surface area. ε_e is set to 1 to simulate a vacuum or air environment. The light source in this simulation is set as a plane wave vertically hitting the plane, which means electron displacement will only happen along the plane. Therefore only the dielectric function along the plane is considered. A schematic is shown to clarify the simulation process (Figure 3-6).

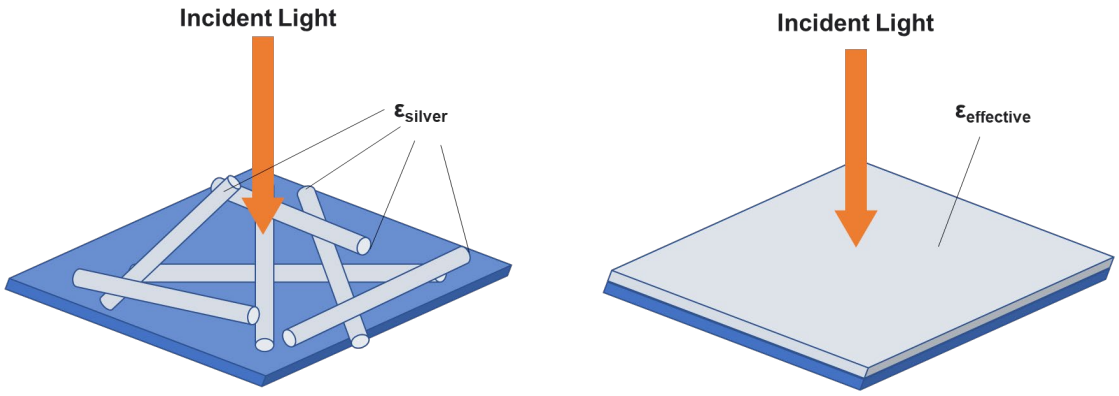

Figure 3-6: A uniformly distributed AgNW-air matrix (a) with ε_{silver} and (b) ε_{air}. By applying the Maxwell Mixing Rule, an approximated homogenized layer with $\varepsilon_{effective}$ was established. The light source is vertical to the plane, so only the dielectric function along the plane is considered.

The optical parameters are brought into the FDTD simulation software to derive the reflectivity. Since the thinnest AgNW diameter that can be mass-produced at present is about 30 nm, the minimum diameter of this simulation is 25 nm. The fill factors of AgNW arrays with diameters of 25 nm, 50 nm, and 100 nm were 0.8, 0.2, and 0.05 to ensure the same quantity of silver used in the arrays. Figure 3-7 is the simulation result; the wavelength range is limited between 400 nm and 12 μm. It can be clearly seen that the reflectivity of the silver array decreases as the diameter increases. This means that increasing the number of AgNWs can increase the reflectivity of light more effectively than increasing the reflectivity of the individual nanowires (diameter increase). Choosing AgNWs with a smaller diameter can bring higher reflectivity under the same silver quantity and thus have better infrared stealth performance.

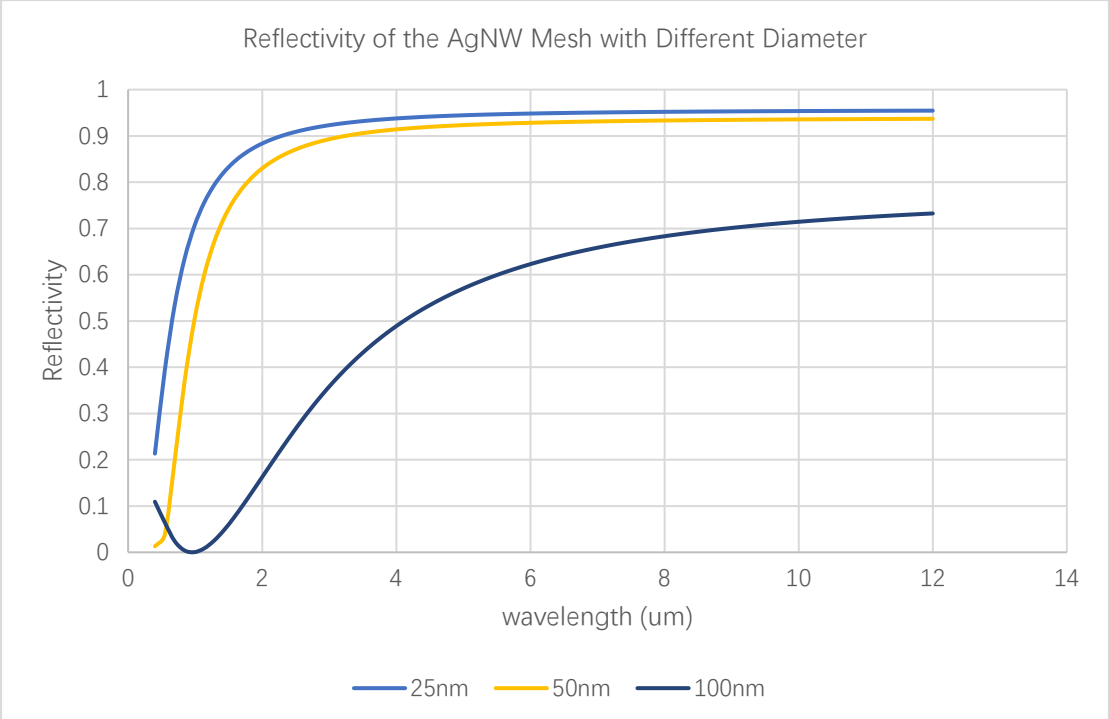

Figure 3-7: Simulation of the AgNWs reflectivity with different diameters. The fill factor is chosen so that the total mass of silver is the same in each network.

3.2.2 Study about Nanowire Junction Fusion

Metal conductivity and light reflectivity are often considered to be related. The Hagen-Rubens approximation describes the relationship between the reflectivity and conductivity of a metal

or metal-like material [83]. It can be seen from Formula 10 that when the conductivity increases, the reflectivity increases:

$$R \approx 1 - 2\sqrt{\frac{2\epsilon_0 \omega}{\sigma}} \tag{10}$$

where R is the reflectivity of the metal, ε_0 is the dielectric function of vacuum, ω is the frequency of the electromagnetic wave, and σ is the DC conductivity of the metal. This suggests that both conductivity and reflectivity depend to some extent on the electron's delocalization degree and the number of delocalized electrons. It is worth noting that this approximation is only valid in wavelengths around LWIR and beyond.

The curing of a AgNW network, such as through thermal annealing, can fuse the overlapping nanowire-nanowire junctions, reducing the junction resistance and thereby achieving higher electrical conductivity of the network. The reduction of the resistance of AgNW networks by curing has been proved by many previous studies [84]. If the decrease in resistivity caused by the fusion of junctions can improve the reflectivity of AgNW arrays, it means that we can increase the infrared stealth performance without increasing the amount of AgNWs. Also, new curing methods that can be applied at room temperature are preferred since many fabrics cannot tolerate high temperatures. Therefore, I experimentally explored the effect of curing AgNWs on reflectivity and conductivity.

3.2.2.1 Experimental procedure

Four 2.5 x 5 cm sized glass substrates are Meyer rod coated (RDS #12) with commercially sourced AgNWs in ethanol two times. The diameter and concentration of the AgNW are 30 nm and 2 mg/mL, respectively. 60 μL of the solution was used for each coating. Samples were left in the open air for 5 minutes for ethanol evaporation. Sheet resistance was measured by a four-point probe (Ossila, Sheffield, United Kingdom). Measurements were taken at four edges and the center point of the sample for experimental stability. Emissivity was measured at the center point of the sample by an ET 10 emissometer. 150 °C was chosen as the annealing temperature since this was found by a groupmate to be the optimal annealing temperature for 30 nm diameter AgNWs [85]. After samples were cured in a low vacuum oven at 150 °C for 15, 30, 45, and 60

mins, the emissivity and sheet resistance were measured again, and the difference was calculated.

3.2.2.2 Results and Discussion

Figure 3-8 describes the change of infrared emissivity and the relative change of sheet resistance when the curing time is 15, 30, 45, and 60 minutes respectively. The resistance value decreases with the prolongation of curing time, but the emissivity does not change significantly. This demonstrates that the decrease in resistivity caused by the fusion of nodes between AgNWs is not related to reflectivity. When a beam of infrared light is incident on the surface of AgNWs, due to the high frequency of electromagnetic waves (about 30 THz), most electrons only vibrate in a single nanowire. So, the fusion of the junction is not effective in increasing reflectivity. When the frequency is reduced to DC (0 Hz), electrons need to pass through many junctions from one end to the other to transmit current. At this time, the reduction of junction resistance caused by node fusion will greatly reduce the resistance value of the AgNW array. In other words, the DC conductivity of AgNW arrays depends not only on the migration of electrons inside an individual AgNWs but also on the hopping between the AgNWs. On the other hand, the reflectivity of the arrays for infrared rays is only related to the vibration of electrons inside an individual nanowire.

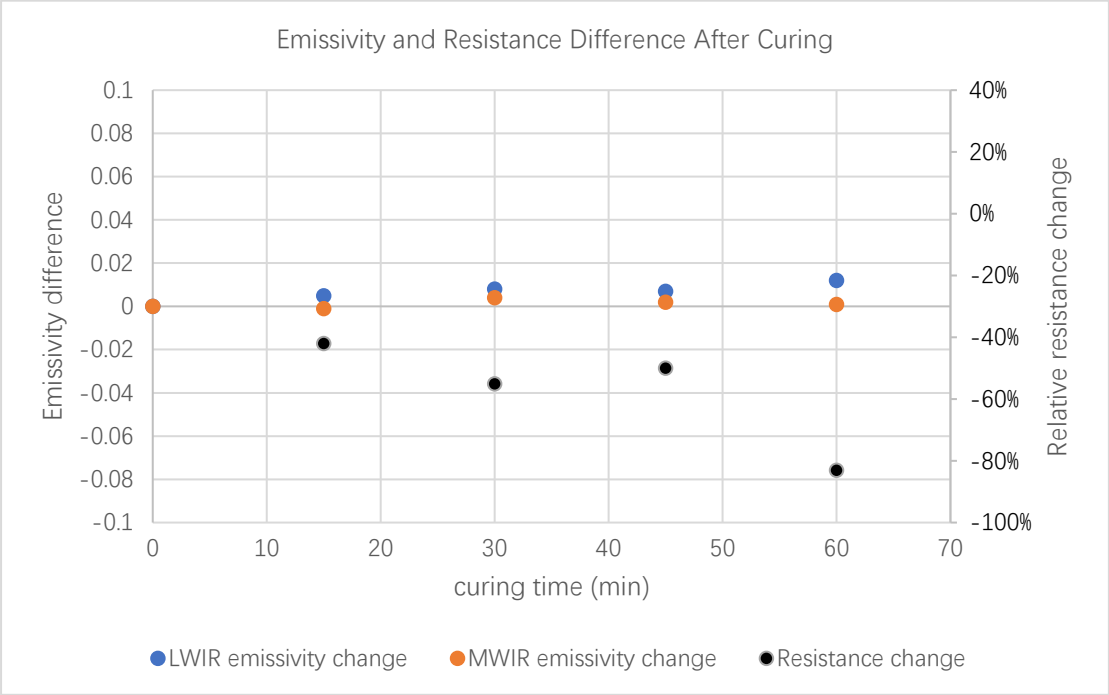

Figure 3-8: Emissivity and resistance change after AgNW curing. Relative resistance change is used since the initial resistance of each sample is different.

A similar situation has also been found in metal-like conductive polymers [86]. The researchers found that doping ethylene glycol (EG) in poly(3,4-ethylenedioxythiophene) polystyrene sulfonate (PEDOT: PSS) can effectively improve the DC conductivity and THz conductivity (0-2.2THz) of PEDOT: PSS(EG) film. But when the electromagnetic wave wavelength is in the visible light-ultraviolet range (100-1000THz), adding EG cannot change the reflectivity. They believe that this is because the light reflection of the film is only related to the transport of electrons in PEDOT nanocrystals, but the improvement of film conductivity depends more on the hopping conduction of electrons between PEDOT nanocrystals. The addition of EG to PEDOT can only make the PEDOT crystals tightly arranged and reduce the barrier of electron transmission between nanocrystals but cannot change the properties (mobility, carrier concentration) inside the crystals, so the reflectivity remains unchanged.

The lack of need for curing is advantageous because many fabrics cannot tolerate temperatures of 150 °C or more which are the optimal temperatures for reducing AgNW network resistance [85]. Thermal curing has also been shown to accelerate AgNW degradation, not only during the anneal but long term as well [87]. According to that study, AgNW instability and corrosion are worsened at elevated temperatures, and higher temperatures also reduce or

remove the polymeric polyvinylpyrrolidone (PVP) layer that typically exists on the surface of the solution-synthesized AgNWs, which otherwise acts as a passivation layer. Lastly, the knowledge that the AgNWs do not need to all be touching and form a connected network has many advantages of its own. For example, it allows for the AgNWs to be mixed with a resin, as will be discussed in the next section.

3.2.3 Agglomeration and Alignment

In the actual fabrication process, the alignment and agglomeration of AgNWs are serious issues that have a bad influence on the infrared stealth efficiency of the fabric. Many studies have shown that the alignment tendency of AgNWs is closely related to the coating direction, where the long axes of the AgNWs tend to be aligned in the same direction as the coating direction [88]. Since it is difficult to change the coating direction of the cloth by 90° in the production line, AgNWs are often arranged along the production direction. And the AgNWs can easily agglomerate during the coating process, especially when the substrate is rough. In order to explore the influence of the agglomeration and alignment of AgNWs on the infrared stealth efficiency of the fabric, I simulated these two phenomena.

3.2.3.1 Simulation Process

Since the Maxwell-Garnett effective medium theory cannot simulate the non-uniform distribution of AgNW arrays effectively, the following simulations use the method of approximating the AgNWs as an intersecting mesh structure. I simulated the agglomeration of AgNWs by adjusting the spacing between AgNWs (figure 3-9). When the distances between the AgNWs are equal, it means that the array is evenly distributed, and if the distances are different, it indicates that the AgNWs are agglomerated. I simulated the alignment of the nanowires by having one case where the AgNWs are arranged in a grid, and another case where all the nanowires are parallel to one another (figure 3-10).

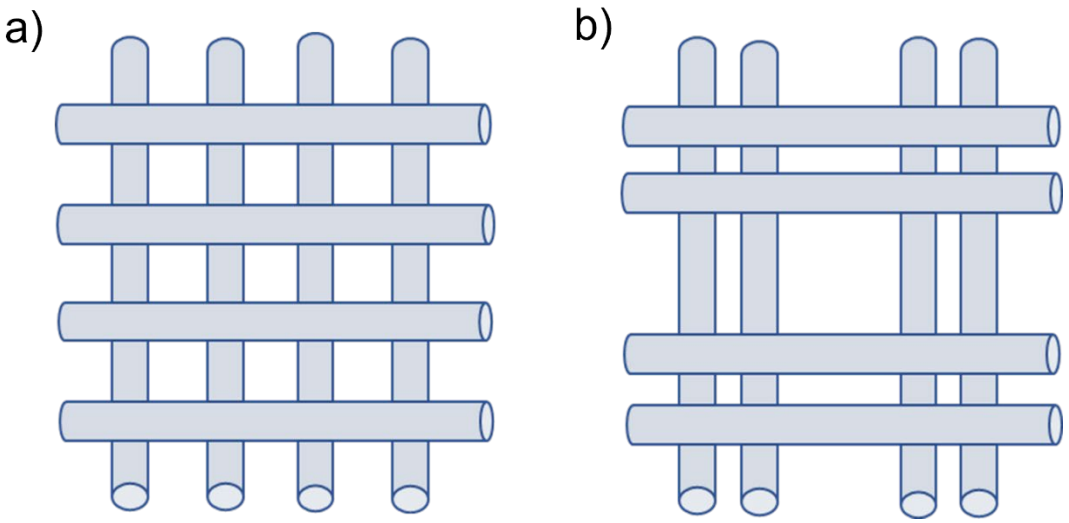

Figure 3-9: Uniformly distributed (a) and agglomerated AgNWs.

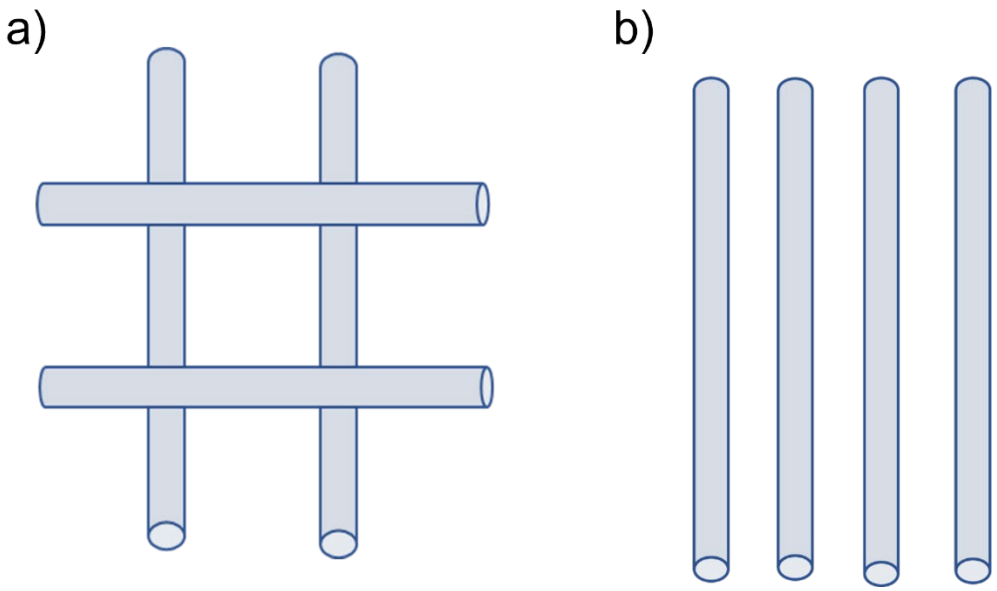

Figure 3-10: Uniformly distributed (a) and fully aligned (b) AgNWs.

3.2.3.2 Results and Discussion

It can be seen from Figure 3-11 (a) that the infrared reflectivity provided by the AgNWs uniformly distributed is much higher. The agglomeration of the AgNWs will significantly weaken the reflectivity in the area with fewer nanowires, so the overall nanowire matrix reflection decreases.

Another finding is that due to the spaces between the AgNWs, the reflectivity slowly increases as the wavelength increases, different from the situation of bulk silver, which has a reflectivity value close to 1 in the visible and infrared range. From Figure 3-11(b), the transmissivity difference in the visible range is slight between uniformly distributed and agglomerated AgNWs, and they are both close to 1. This means that agglomeration will not enormously change the visible characteristics of AgNWs, and a AgNW coating is always relatively transparent to visible light. People can spray different camouflage patterns on the surface of the clothes according to the usage environment, and the final AgNW coating will not cover the original color of the clothes. It is another advantage of using AgNWs as infrared stealth fabric.

It can be seen from Figure 3-12 that the reflectivity of the AgNWs randomly distributed in the plane is much higher than that of the AgNWs arranged in a straight line in the MWIR and LWIR range, which means AgNWs alignment is detrimental to the infrared reflectivity. When the AgNWs are arranged in a straight line, the reflectance-wavelength curve is very similar to the curve described by the Lorentz model. This indicates that when a beam of light is incident on the AgNWs array, if the arrangement tendency of the AgNWs is pronounced, the array will show a property similar to that of a dielectric, and the reflectivity to light will decrease.

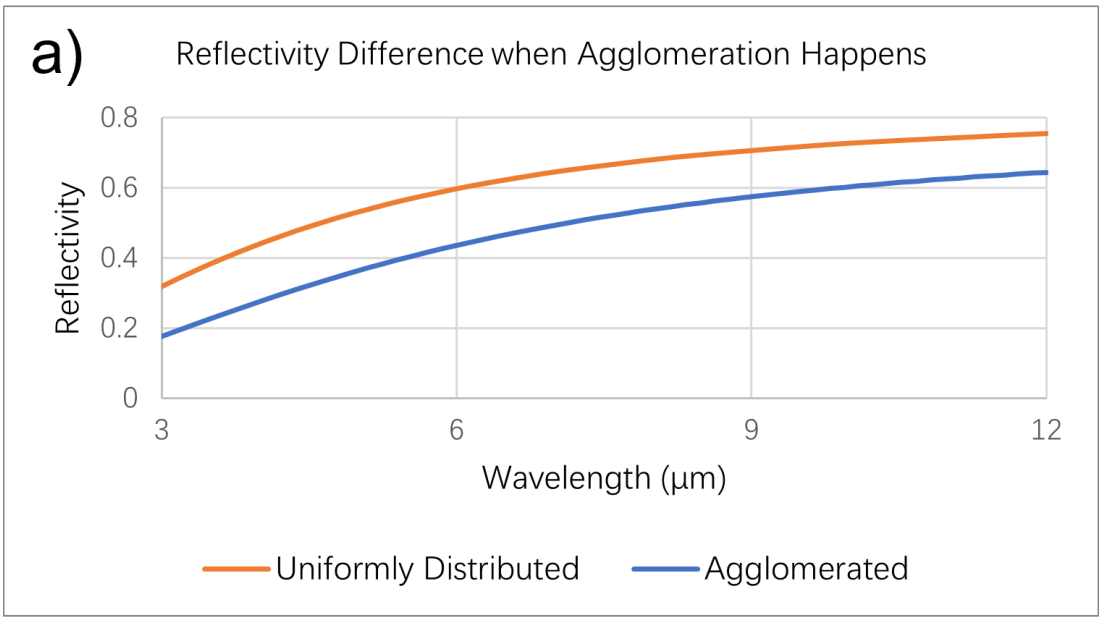

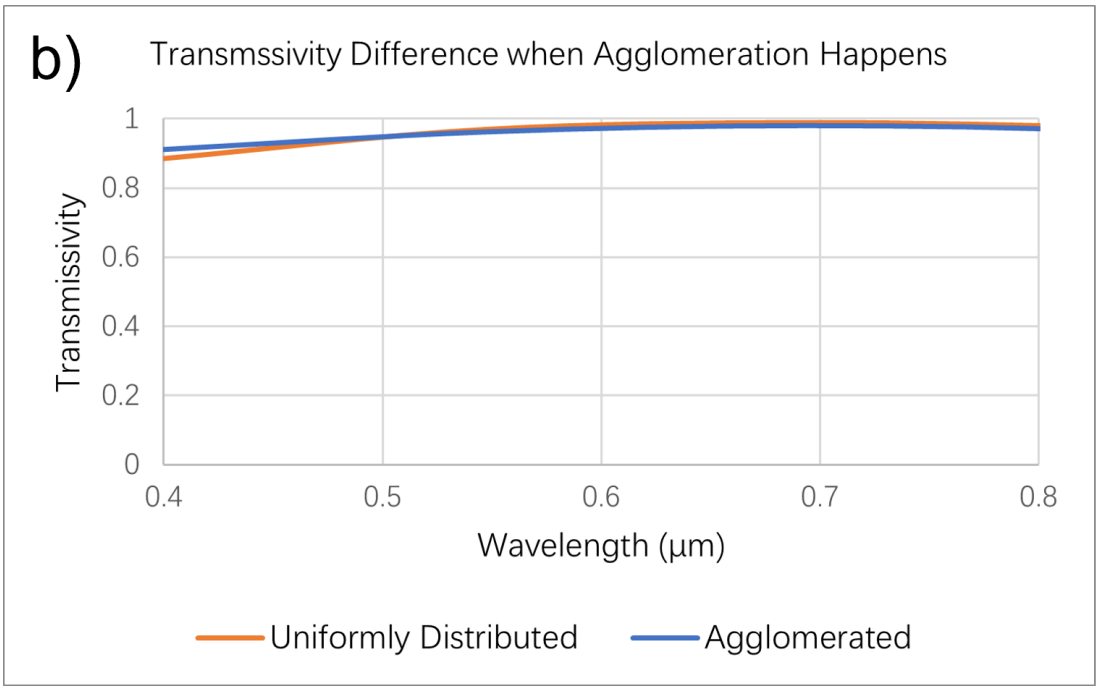

Figure 3-11: (a) Infrared reflectivity difference and (b) visible transmissivity difference of a uniformly distributed AgNW mesh and an agglomerated AgNW mesh.

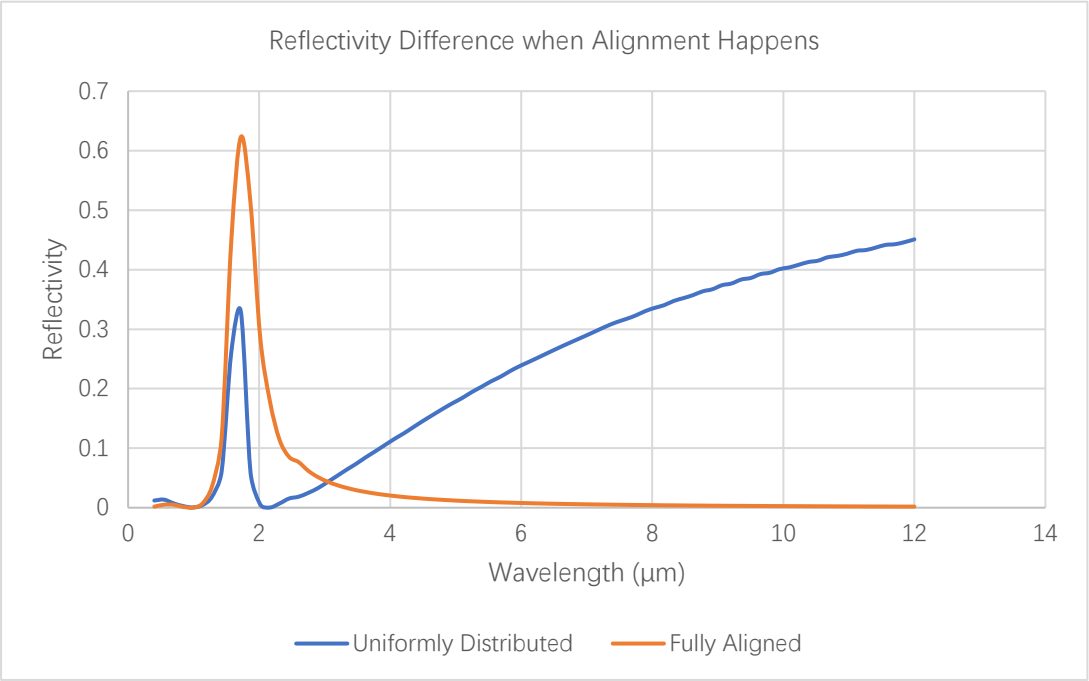

Figure 3-12**: Reflectivity difference of a uniformly distributed AgNW mesh and a fully aligned AgNW grating.**

Through the results from above, agglomeration and alignment of AgNWs phenomena are detrimental to infrared reflection efficiency. Adding a layer of TPU film on the surface of the fabric, as in the previous chapter, to flatten the fabric substrate is one solution to AgNW agglomeration. However, considering that the alignment phenomenon still exists and the negative influence of TPU film on the original properties of the fabric, it is a better choice to mix AgNWs with resin to form a more stable AgNW-resin matrix. The increase of solution viscosity due to the resin can alleviate the AgNW agglomeration and alignment phenomena. The increased viscosity increases the friction between the AgNWs and the fabric, and it is more likely that the nanowires will not be aligned along the coating direction during coating. The dispersion effect of the resin on the AgNW matrix is significant. Choosing an appropriate resin can ensure that AgNW is evenly distributed, and the agglomeration phenomenon is significantly reduced.

Another advantage of using resin is that it can protect nanowires and increase the robustness of the fabric without further treatment while using TPU film requires an additional TPU film to be laminated on the upper sides of the AgNWs. The resin is not conductive and interferes with AgNWs having good electrical contact with other nanowires. However, the

results in subsection 3.2.2 show that the reflectivity of AgNW arrays to infrared light is only related to the vibration of electrons (conductivity) in an individual nanowire. Therefore, the adverse effect of the resin on the conductivity of the AgNW arrays is unimportant.

The organic functional groups in most resins can absorb infrared rays, which may be harmful to the reflectivity of the overall matrix. For example, the stretching vibration of C-N in polyurethane has a strong absorption effect on infrared rays with a wavelength of 9.5 μm [89]. This is disadvantageous for coatings that strive to be infrared reflective. Considering the dispersing effect of resin on AgNWs arrays mentioned above, it is particularly important to optimize the amount and type of resin used. Liu et al. researched the effects of different types of resin on the emissivity performance of an aluminum power-resin matrix [90]. They found that the infrared absorption coefficient of acrylic resin (AR) is lower than that of epoxy resin (ER) and polyurethane resin (PR), but the infrared emissivity of the aluminum-PR is the lowest. This seemingly contradictory result can be explained by the SEM images of the three different coatings. The distribution of aluminum powders of the Al-PR coating is the most uniform, which indicates that the dispersion effect of PR on aluminum powder is the most effective, so the emissivity of the final coating is the lowest.

In summary, a resin that has a better dispersion effect and can control the solution viscosity while having a weaker absorption of infrared rays will be beneficial to the infrared stealth efficiency of the coating.

3.3 Conclusion

In this chapter, AgNWs were considered to be a suitable material for the preparation of infrared stealth fabric coatings due to its high infrared stealth efficiency, good matching with the fabric substrate, and low influence on the properties of the fabric. Through simulation, AgNWs with smaller diameters have a better infrared stealth effect under the same mass loading. Although curing reduces the electrical resistance of AgNW arrays, it has no obvious effect on infrared reflectivity. This shows that the infrared reflection of the AgNW array depends more on the vibration of electrons in a single nanowire than on the movement between nanowires. Adding resin to AgNWs to reduce alignment and agglomeration may effectively improve the infrared

reflectivity of AgNW arrays. However, it should be noted that the resin also absorbs infrared rays. It is therefore important to strike a balance between the two factors.

Chapter 4

Conclusions and Future Work

4.1 Conclusions

Different from most of the current research that only aimed at improving the functionality of smart textiles, the main innovation of this work lies in the investigation of the original properties of fabrics. Two representative smart textiles, e-textiles and infrared stealth fabric are studied and optimized in this work. By optimizing the selection of materials and the preparation process, the performance of smart textiles is improved while the wearability is considered simultaneously. This work provides guidance for future research on these two and similar smart textiles.

In Chapter 2, the effects of different TPU films on the performance of e-textiles are studied and discussed in detail, which has never been done before in the literature. Firstly, the TPU film was proved to be necessary in the preparation of e-textiles, because direct printing of commercial conductive inks on the fabric surface causes the samples to be unable to withstand slight tension. An increase in the thickness of the TPU film will reduce the drape, breathability, and thermal permeance of the fabric, but at the same time, will improve the electrical conductivity and stretchability of the fabric. The buffer and insulation function of the TPU film is considered to be the key to improving the electrical properties of the fabric. The effect of different types of TPU films on the fabric was also studied in detail, where density and number of layers were the two studied variables. Lower density TPU film can significantly improve the drape and breathability of the fabric without damaging the typical properties of the fabric. Compared with single-layer TPU film, the use of double-layered TPU film can improve the conductivity and stretchability of e-textiles. This is because the upper printing layer has a higher melting point and has a better insulation effect on the conductive layer and the fabric. Finally, processing conditions were investigated to further enhance the performance of e-textiles. Increasing the curing temperature can effectively reduce the resistance of the silver layer, but temperatures exceeding the melting point of the TPU film are undesirable. The increase of hot-

pressing temperature and time can effectively improve the conductivity and stretchability of e-textiles and has little adverse effect on the breathability and thermal performance of e-textiles.

In Chapter 3, because AgNWs have the advantages of high infrared stealth efficiency, good matching with the fabric substrate, and little influence on the fabric properties, it is selected as the functional substance of the new infrared stealth coating. AgNW coating solves the shortcomings of high infrared emissivity and severe influence on the original properties of fabrics. When optimizing the parameters of AgNWs, the results show that AgNWs with smaller diameters have a better infrared stealth effect under the same mass loading. When further optimizing the formulation of the AgNW solution, resin is postulated to be able to effectively reduce the agglomeration and alignment of the array, thus making the array closer to a random distribution, which should improve its infrared reflectivity. However, resin also absorbs infrared rays, resulting in a decrease in the reflectivity of the coating, so it is important to control the amount of resin used to achieve the minimum emissivity. When optimizing the curing conditions, it was found that increasing the curing time did not significantly affect the infrared reflectivity of the AgNW arrays but could increase the conductivity of the arrays. This reveals the mechanism of the AgNW array as an infrared stealth material, namely that the vibration of electrons in a single nanowire determines its stealth performance.

4.2 Future Work

Chapter 2 uses a variety of commercial TPU films and discusses the influence of TPU films on the performance of e-textiles. In the future, if the research can start from the synthesis of TPU film, it will be of great help to further reveal the mechanism of the TPU film functions. For example, the density of the film can be customized, which can better explain the inflection point in Figure 2-5(c). The raw materials and processing history would also be known as opposed to that of commercial TPU films.

The samples in the e-textile study only contain conductive traces, and the difference in the functionality of e-textiles may lead to a difference in the required TPU film. For example, for a strain sensor, the residual strain needs to be reduced as much as possible to ensure the accuracy of the sensor. Then the optimized thickness of the TPU film should be smaller;

otherwise, the residual strain will increase significantly. Future research can optimize the TPU film for e-textiles with different functions.

Another direction for future work is to use other strategies to minimize the impact of the TPU on the textile, such as cutting holes in the TPU layer between circuitries.

Chapter 3 proposes a new formula for infrared stealth fabrics to include AgNWs and resins. Future work can start from adding additives and the selection of new functional substances.

Although the use of additives cannot directly improve the infrared stealth performance of textiles, its effects in other aspects, such as improving the wear resistance of fabrics and reducing preparation costs, are very important. Due to the environmental protection requirements of the textile industry, AgNW solutions are often aqueous. The current commercially available aqueous AgNW solution has a low concentration due to stability reasons, so infrared stealth textiles often need to be coated with the solution multiple times to achieve the required stealthing performance. Thickening agents can maintain a uniform and stable suspension state by increasing the viscosity of the solution. Adding thickener to the formula can effectively increase the concentration of AgNWs in the solution, simplify the fabrication process of textiles, and shorten the preparation time. The downside of thickeners is that the evenness of the coating may be reduced due to the drastic change in the solution viscosity.

In addition to improving the stealth performance of the AgNW array, the resin can also improve the wear resistance of the fabric, which is achieved through the crosslinking between the resin molecular chains. The use of an appropriate crosslinking agent can effectively promote the occurrence of the crosslinking process and greatly improve the wear resistance of the fabric. But it is worth noting that excessive crosslinking will reduce the drape of the fabric. In future work, if the type and dosage of additives can be explored, the formula of infrared stealth coating can be further optimized, making the formulation a more mature product.

For the selection of functional substances, silver nanoflakes (as opposed to silver microflakes discussed in Chapter 3) are promising. Its infrared stealth efficiency may exceed that of AgNWs because of the smaller size effect. And the edge length of nanoflakes is much

smaller than the diameter of a fiber, making it possible to conformally cover a fiber. The haze problem does not exist if the nanoflakes can be tightly packed on the fiber surface. Future work can start from the synthesis of stable water-based silver nanoflake solution and the stealth properties of these nanoflakes should be tested and compared with the current AgNWs solution. It will provide a potential new option for the coating of infrared stealth fabrics.

Bibliography

[1] Çelikel, D. C. Smart E-Textile Materials. *Advanced Functional Materials* **2020**. https://doi.org/10.5772/intechopen.92439.

[2] Sarif Ullah Patwary, M. S. Smart Textiles and Nano-Technology: A General Overview. *Journal of Textile Science & Engineering* **2015**, *05* (01). https://doi.org/10.4172/2165-8064.1000181.

[3] Galante, A. J.; Haghanifar, S.; Romanowski, E. G.; Shanks, R. M. Q.; Leu, P. W. Superhemophobic and Antivirofouling Coating for Mechanically Durable and Wash-Stable Medical Textiles. *ACS Applied Materials & Interfaces* **2020**, *12* (19), 22120–22128. https://doi.org/10.1021/acsami.9b23058.

[4] Kicklighter, T. H.; Edsall, J. R.; Martin, M. Effect of Moisture-Wicking Garments on Temperature Regulation during Exercise. *International Journal of Athletic Therapy and Training* **2011**, *16* (6), 9–13. https://doi.org/10.1123/ijatt.16.6.9.

[5] Aravind H. Patil; Jadhav, S. A.; More, V. B.; Sonawane, K. D.; Patil, P. S. Novel One Step Sonosynthesis and Deposition Technique to Prepare Silver Nanoparticles Coated Cotton Textile with Antibacterial Properties. *Colloid Journal* **2019**, *81* (6), 720–727. https://doi.org/10.1134/s1061933x19070019.

[6] Shams-Ghahfarokhi, F.; Khoddami, A.; Mazrouei-Sebdani, Z.; Rahmatinejad, J.; Mohammadi, H. A New Technique to Prepare a Hydrophobic and Thermal Insulating Polyester Woven Fabric Using Electro-Spraying of Nano-Porous Silica Powder. *Surface and Coatings Technology* **2019**, *366*, 97–105. https://doi.org/10.1016/j.surfcoat.2019.03.025.

[7] Mondal, S. Phase Change Materials for Smart Textiles – an Overview. *Applied Thermal Engineering* **2008**, *28* (11-12), 1536–1550. https://doi.org/10.1016/j.applthermaleng.2007.08.009.

[8] Ramlow, H.; Andrade, K. L.; Immich, A. P. S. Smart Textiles: An Overview of Recent Progress on Chromic Textiles. *The Journal of The Textile Institute* **2020**, 1–20. https://doi.org/10.1080/00405000.2020.1785071.

[9] Gök, M. O.; Bilir, M. Z.; Gürcüm, B. H. Shape-Memory Applications in Textile Design. *Procedia - Social and Behavioral Sciences* **2015**, *195*, 2160–2169. https://doi.org/10.1016/j.sbspro.2015.06.283.

[10] Zhou, Z.; Padgett, S.; Cai, Z.; Conta, G.; Wu, Y.; He, Q.; Zhang, S.; Sun, C.; Liu, J.; Fan, E.; Meng, K.; Lin, Z.; Uy, C.; Yang, J.; Chen, J. Single-Layered Ultra-Soft Washable Smart Textiles for All-around Ballistocardiograph, Respiration, and Posture Monitoring during Sleep. *Biosensors and Bioelectronics* **2020**, *155*, 112064. https://doi.org/10.1016/j.bios.2020.112064.

[11] Liu, Y. W.; Gorgutsa, S.; Santato, C.; Maksim Skorobogatiy. Flexible, Solid Electrolyte-Based Lithium Battery Composed of $LiFePO_4$Cathode and $Li_4Ti_5O_{12}$Anode for Applications in Smart Textiles. *Journal of the Electrochemical Society* **2012**, *159* (4), A349–A356. https://doi.org/10.1149/2.020204jes.

[12] Choi, S.; Jo, W.; Jeon, Y.; Kwon, S.; Kwon, J. H.; Son, Y. H.; Kim, J.; Park, J. H.; Kim, H.; Lee, H. S.; Nam, M.; Jeong, E. G.; Bin Shin, J.; Kim, T.-S.; Choi, K. C. Multi-Directionally Wrinkle-Able Textile OLEDs for Clothing-Type Displays. *npj Flexible Electronics* **2020**, *4* (1). https://doi.org/10.1038/s41528-020-00096-3.

[13] Markets, R. and. *Global Smart Textiles Market Opportunities and Strategies to 2031: North America was the Largest Region in 2021*. GlobeNewswire News Room.https://www.globenewswire.com/en/news-release/2023/04/04/2640431/28124/en/Global-Smart-Textiles-Market-Opportunities-and-Strategies-to-2031-North-America-was-the-Largest-Region-in-2021.html (accessed 2023-07-22).

[14] Li, J.; Tian, X.; Hua, T.; Fu, J.; Koo, M.; Chan, W.; Poon, T. Chitosan Natural Polymer Material for Improving Antibacterial Properties of Textiles. *ACS Applied Bio Materials* **2021**. https://doi.org/10.1021/acsabm.1c00078.

[15] Marvin, C. *When Old Technologies Were New : Thinking about Electric Communication in the Late Nineteenth Century*; Oxford University Press: New

York, 1988.

[16] Koncar, V.; Manchester, I. *Smart Textiles and Their Applications*; Woodhead Pub. ; [Manchester, England: Amsterdam, 2016.

[17] Xiang, S.; Zhang, N.; Fan, X. From Fiber to Fabric: Progress towards Photovoltaic Energy Textile. *Advanced Fiber Materials* **2021**, *3* (2), 76–106. https://doi.org/10.1007/s42765-020-00062-8.

[18] Vu, C. C.; Kim, S. J.; Kim, J. Flexible Wearable Sensors - an Update in View of Touch-Sensing. *Science and Technology of Advanced Materials* **2021**. https://doi.org/10.1080/14686996.2020.1862629.

[19] Cardenas, A. F.; Pon, R. K.; Cameron, R. B. Management of Streaming Body Sensor Data for Medical Information Systems. **2003**, 186–191.

[20] Patron, D.; Mongan, W. M.; Kurzweg, T. P.; Fontecchio, A. K.; Dion, G.; Anday, E. K.; Dandekar, K. R. On the Use of Knitted Antennas and Inductively Coupled RFID Tags for Wearable Applications. *IEEE Transactions on Biomedical Circuits and Systems* **2016**, *10* (6), 1047–1057. https://doi.org/10.1109/tbcas.2016.2518871.

[21] Komolafe, A.; Zaghari, B.; Torah, R.; Weddell, A. S.; Khanbareh, H.; Tsikriteas, Z. M.; Vousden, M.; Wagih, M.; Jurado, U. T.; Shi, J.; Yong, S.; Arumugam, S.; Li, Y.; Yang, K.; Savelli, G.; White, N. M.; Beeby, S. E-Textile Technology Review-from Materials to Application. *IEEE Access* **2021**, *9*, 97152–97179. https://doi.org/10.1109/ACCESS.2021.3094303.

[22] Song, H. -Y.; Lee, J. -H.; Kang, D.; Cho, H.; Cho, H. -S.; Lee, J. -W.; Lee, Y. -J. Textile Electrodes of Jacquard Woven Fabrics for Biosignal Measurement. *Journal of the Textile Institute* **2010**, *101* (8), 758–770. https://doi.org/10.1080/00405000903442086.

[23] Fobelets, K.; Thielemans, K.; Mathivanan, A.; Papavassiliou, C. Characterization of Knitted Coils for E-Textiles. *IEEE Sensors Journal* **2019**, *19* (18), 7835–7840. https://doi.org/10.1109/JSEN.2019.2917542.

[24] Linz, T.; Kallmayer, C.; Aschenbrenner, R.; Reichl, H. Fully Untegrated EKG

Shirt Based on Embroidered Electrical Interconnections with Conductive Yarn and Miniaturized Flexible Electronics. **2006**. https://doi.org/10.1109/bsn.2006.26.

[25] Takamatsu, S.; Kobayashi, T.; Shibayama, N.; Miyake, K.; Itoh, T. Fabric Pressure Sensor Array Fabricated with Die-Coating and Weaving Techniques. *Sensors and Actuators A-physical* **2012**, *184*, 57–63. https://doi.org/10.1016/j.sna.2012.06.031.

[26] Ginestet, G.; Brechet, N.; Torres, J.; Moradi, E.; Ukkonen, L.; Bjorninen, T.; Virkki, J. Embroidered Antenna-Microchip Interconnections and Contour Antennas in Passive UHF RFID Textile Tags. *IEEE Antennas and Wireless Propagation Letters* **2017**, *16*, 1205–1208. https://doi.org/10.1109/lawp.2016.2628086.

[27] Komolafe, A.; Torah, R.; Wei, Y.; Nunes-Matos, H.; Li, M.; Hardy, D.; Dias, T.; Tudor, M.; Beeby, S. Integrating Flexible Filament Circuits for E-Textile Applications. *Advanced Materials Technologies* **2019**, *4* (7), 1900176. https://doi.org/10.1002/admt.201900176.

[28] Yang, K.; Torah, R.; Wei, Y.; Beeby, S.; Tudor, J. Waterproof and Durable Screen Printed Silver Conductive Tracks on Textiles. *Textile Research Journal* **2013**, *83* (19), 2023–2031. https://doi.org/10.1177/0040517513490063.

[29] de Vos, M.; Torah, R.; Tudor, J. Dispenser Printed Electroluminescent Lamps on Textiles for Smart Fabric Applications. *Smart Materials and Structures* **2016**, *25* (4), 045016. https://doi.org/10.1088/0964-1726/25/4/045016.

[30] Almusallam, A.; Torah, R. N.; Zhu, D.; Tudor, M. J.; Beeby, S. P. Screen-Printed Piezoelectric Shoe-Insole Energy Harvester Using an Improved Flexible PZT-Polymer Composites. *Journal of Physics: Conference Series* **2013**, *476*, 012108. https://doi.org/10.1088/1742-6596/476/1/012108.

[31] Chauraya, A.; Tudor, J.; Vardaxoglou, J. C.; Torah, R.; Li, Y.; Whittow, W. G.; Beeby, S.; Yang, K. Inkjet Printed Dipole Antennas on Textiles for Wearable Communications. *IET Microwaves, Antennas & Propagation* **2013**, *7* (9), 760–767. https://doi.org/10.1049/iet-map.2013.0076.

[32] Kim, Y.-S.; Kim, H.-J.; Yoo, H.-J. Electrical Characterization of Screen-Printed Circuits on the Fabric. **2010**, *33* (1), 196–205. https://doi.org/10.1109/tadvp.2009.2034536.

[33] Zhou, Y.; Soltani, S.; Li, B. M.; Wu, Y.; Kim, I.-H.; Soewardiman, H.; Werner, D. H.; Jur, J. S. Direct-Write Spray Coating of a Full-Duplex Antenna for E-Textile Applications. **2020**, *11* (12), 1056–1056. https://doi.org/10.3390/mi11121056.

[34] Hong, H.; Jiyong, H.; Moon, K.-S.; Yan, X.; Wong, C. Rheological Properties and Screen Printability of UV Curable Conductive Ink for Flexible and Washable E-Textiles. *Journal of Materials Science & Technology* **2021**, *67*, 145–155. https://doi.org/10.1016/j.jmst.2020.06.033.

[35] Du, D.; Yang, X.; Yang, Y.; Zhao, Y.; Wang, Y. Silver Nanowire Ink for Flexible Circuit on Textiles. *Micromachines* **2019**, *10* (1), 42. https://doi.org/10.3390/mi10010042.

[36] Duan, Q.; Lan, B.; Lu, Y. Highly Dispersed, Adhesive Carbon Nanotube Ink for Strain and Pressure Sensors. **2022**, *14* (1), 1973–1982. https://doi.org/10.1021/acsami.1c20133.

[37] Farraj, Y.; Kanner, A.; Magdassi, S. E-Textile by Printing an All-through Penetrating Copper Complex Ink. *ACS Applied Materials & Interfaces* **2023**, *15* (17), 21651–21658. https://doi.org/10.1021/acsami.3c02242.

[38] Islam, T.; Goodman, S.; Schleif, N.; Mary Ellen Berglund; Zacharias, C.; Compton, C.; Dunne, L. E. Surface-Mount Manufacturing for E-Textile Circuits. **2017**. https://doi.org/10.1145/3123021.3123058.

[39] Ma, F.; Lin, Y.; Yuan, W.; Ding, C.; Su, W.; Meng, X.; Cui, Z. Fully Printed, Large-Size Alternating Current Electroluminescent Device on Fabric for Wearable Textile Display. *ACS Applied Electronic Materials* **2021**, *3* (4), 1747–1757. https://doi.org/10.1021/acsaelm.1c00039.

[40] Merilampi, S.; Björninen, T.; Haukka, V.; Ruuskanen, P.; Ukkonen, L.; Sydänheimo, L. Analysis of Electrically Conductive Silver Ink on Stretchable Substrates under Tensile Load. *Microelectronics Reliability* **2010**, *50* (12), 2001–

2011. https://doi.org/10.1016/j.microrel.2010.06.011.

[41] Yokus, M. A.; Foote, R.; Jur, J. S. Printed Stretchable Interconnects for Smart Garments: Design, Fabrication, and Characterization. *IEEE Sensors Journal* **2016**, *16* (22), 7967–7976. https://doi.org/10.1109/jsen.2016.2605071.

[42] Casson, L. *Ships and Seamanship in the Ancient World*; Princeton University Press, 1986.

[43] Hu, J.; Hu, Y.; Ye, Y.; Shen, R. Unique Applications of Carbon Materials in Infrared Stealth: A Review. *Chemical Engineering Journal* **2023**, *452*, 139147. https://doi.org/10.1016/j.cej.2022.139147.

[44] Belliveau, R. G.; DeJong, S. A.; Boltin, N. D.; Lu, Z.; Cassidy, B. M.; Morgan, S. L.; Myrick, M. Mid-Infrared Emissivity of Nylon, Cotton, Acrylic, and Polyester Fabrics as a Function of Moisture Content. *Textile Research Journal* **2019**, *90* (13-14), 1431–1445. https://doi.org/10.1177/0040517519888825.

[45] https://baike.baidu.com/item/%E7%BA%A2%E5%A4%96%E9%9A%90%E8%BA%AB%E6%8A%80%E6%9C%AF/6048599#reference-2-5945603-wrap (accessed 2023-07-28).

[46] Aftab; Khan, A.; Asiri, A. M.; Mohammad Omaish Ansari; Amsterdam, E. *Advances in Aerogel Composites for Environmental Remediation*; Elsevier Inc., Copyright: Amsterdam ; Oxford ; Cambridge, Ma, 2021.

[47] Kirchhoff, G. Ueber Das Verhältniss Zwischen Dem Emissionsvermögen Und Dem Absorptionsvermögen Der Körper Für Wärme Und Licht. *Annalen der Physik und Chemie* **1860**, *185* (2), 275–301. https://doi.org/10.1002/andp.18601850205.

[48] Xu, R.; Wang, W.; Yu, D. A Novel Multilayer Sandwich Fabric-Based Composite Material for Infrared Stealth and Super Thermal Insulation Protection. *Composite Structures* **2019**, *212*, 58–65. https://doi.org/10.1016/j.compstruct.2019.01.032.

[49] Jia, L.; Fu, B.; Lu, M.; Liang Hui-e; Wang, L. High-Performance Aramid Fabric in Infrared Shielding by Magnetron Sputtering Method. **2020**, *7* (5), 056401–056401. https://doi.org/10.1088/2053-1591/ab8b1c.

[50] Peng, L.; Jiang, S. Q.; Guo, R.; Xu, J.; Li, X.; Miao, D.; Wang, Y. IR Protection Property and Color Performance of TiO2/Cu/TiO2 Coated Polyester Fabrics. **2018**, *29* (19), 16188–16198. https://doi.org/10.1007/s10854-018-9708-6.

[51] Granqvist, C. G. Solar Energy Materials. *Advanced Materials* **2003**, *15* (21), 1789–1803. https://doi.org/10.1002/adma.200300378.

[52] Wang, K.; Wang, C.; Yin, Y.; Chen, K. Modification of al Pigment with Graphene for Infrared/Visual Stealth Compatible Fabric Coating. *Journal of Alloys and Compounds* **2017**, *690*, 741–748. https://doi.org/10.1016/j.jallcom.2016.08.171.

[53] Maria Cristina Larciprete; Paoloni, S.; R. Li Voti; Yves-Simon Gloy; Sibilia, C. Infrared Radiation Characterization of Several Stainless Steel Textiles in the 3.5–5.1 Mm Infrared Range. **2018**, *132*, 168–173. https://doi.org/10.1016/j.ijthermalsci.2018.04.024.

[54] Mao, Z.; Yu, X.; Zhang, L.; Zhong, Y.; Xu, H. Novel Infrared Stealth Property of Cotton Fabrics Coated with Nano ZnO: (Al, La) Particles. **2014**, *104*, 111–115. https://doi.org/10.1016/j.vacuum.2014.01.011.

[55] Yu, X.; Lin Ping Zhang; Zhong, Y.; Xu, H.; Zhi Ping Mao. Effect of La Content on the Infrared Stealth Property of ZnO: (La, Al) Coated on Cotton Fabrics. **2014**, *692*, 337–340. https://doi.org/10.4028/www.scientific.net/amm.692.337.

[56] Yu, X. L.; Zhang, L. P.; Zhong, Y.; Xu, H.; Mao, Z. P. Novel Infrared Stealth Properties of Cotton Fabric with ZnO: (Al, In) Coating. *Advanced Materials Research* **2014**, *936*, 1031–1034. https://doi.org/10.4028/www.scientific.net/amr.936.1031.

[57] Yu, Z.; Yang, N.; Apostolopoulou-Kalkavoura, V.; Qin, B.; Ma, Z.; Xing, W.; Qiao, C.; Bergström, L.; Antonietti, M.; Yu, S. Fire-Retardant and Thermally Insulating Phenolic-Silica Aerogels. *Angewandte Chemie* **2018**, *130* (17), 4628–4632. https://doi.org/10.1002/ange.201711717.

[58] Wang, W. R. J.; Fang, S.; Zhang, L.; Mao, Z. Infrared Stealth Property Study of Mesoporous Carbon-Aluminum Doped Zinc Oxide Coated Cotton Fabrics. *Textile Research Journal* **2014**, *85* (10), 1065–1075.

https://doi.org/10.1177/0040517514559586.

[59] Gu, J.; Wang, W.; Yu, D. Temperature Control and Low Infrared Emissivity Double-Shell Phase Change Microcapsules and Their Application in Infrared Stealth Fabric. *Progress in Organic Coatings* **2021**, *159*, 106439. https://doi.org/10.1016/j.porgcoat.2021.106439.

[60] Zhou, X.; Xin, B.; Chen, Z.; Peng, X.; Zhuo, T.; Yu, J. Preparation of PANI-Coated Hollow Glass Microsphere and Its Application in Dual-Band Stealth Coated Fabric. *Polymer Bulletin* **2021**, *79* (9), 7555–7570. https://doi.org/10.1007/s00289-021-03854-z.

[61] Mao, Z.; Wang, W.; Liu, Y.; Zhang, L.; Xu, H.; Zhong, Y. Infrared Stealth Property Based on Semiconductor (M)-To-Metallic (R) Phase Transition Characteristics of W-Doped VO2 Thin Films Coated on Cotton Fabrics. *Thin Solid Films* **2014**, *558*, 208–214. https://doi.org/10.1016/j.tsf.2014.02.055.

[62] Ergoktas, M. S.; Bakan, G.; Steiner, P.; Bartlam, C.; Malevich, Y.; Ozden-Yenigun, E.; He, G.; Karim, N.; Cataldi, P.; Bissett, M. A.; Kinloch, I. A.; Novoselov, K. S.; Kocabas, C. Graphene-Enabled Adaptive Infrared Textiles. *Nano Letters* **2020**, *20* (7), 5346–5352. https://doi.org/10.1021/acs.nanolett.0c01694.

[63] Salihoglu, O.; Uzlu, H. B.; Yakar, O.; Aas, S.; Balci, O.; Kakenov, N.; Balci, S.; Olcum, S.; Süzer, S.; Kocabas, C. Graphene-Based Adaptive Thermal Camouflage. *Nano Letters* **2018**, *18* (7), 4541–4548. https://doi.org/10.1021/acs.nanolett.8b01746.

[64] Wang, W.; Zhang, L.; Liu, Y.; Xu, H.; Zhong, Y.; Mao, Z. Synthesis and Infrared Stealth Property of Ordered Mesoporous Carbon–Aluminum-Doped Zinc Oxide Composites. **2013**, *52* (43), 15066–15074. https://doi.org/10.1021/ie401827s.

[65] Xu, T.; Goldthorpe, I. A. Mitigating the Impact of Thermoplastic Polyurethane Films on the Performance of Electronic Textiles. **2022**. https://doi.org/10.1109/ifetc53656.2022.9948436.

[66] Method for Determination of bending length and flexural rigidity of fabrics, British Standard

3356, 1990.

[67] Standard Test Methods for Water Vapor Transmission of Organic Coating Films, ASTM D1653-13, 2021.

[68] Bai, L.; Zhao, X.; Bao, R.-Y.; Liu, Z.-Y.; Yang, M.-B.; Yang, W. Effect of Temperature, Crystallinity and Molecular Chain Orientation on the Thermal Conductivity of Polymers: A Case Study of PLLA. *Journal of Materials Science* **2018**, *53* (14), 10543–10553. https://doi.org/10.1007/s10853-018-2306-4.

[69] Ataeefard, M. Influence of Paper Surface Characteristics on Digital Printing Quality. *Surface Engineering* **2014**, *30* (7), 529–534. https://doi.org/10.1179/1743294414y.0000000264.

[70] Muhammed KayaharmanElectron. Mater.; Argasinski, H.; Atkinson, J.; Zhang, K.; Zhou, Y.; Goldthorpe, I. A. Enhancing and Understanding the High Stretchability of Printable, Conductive Silver Nanowire Ink. *J. Electron. Mater.* **2023**, *52* (7), 4634–4643. https://doi.org/10.1007/s11664-023-10417-7.

[71] Tokuno, T.; Nogi, M.; Karakawa, M.; Jiu, J.; Nge, T. T.; Aso, Y.; Suganuma, K. Fabrication of Silver Nanowire Transparent Electrodes at Room Temperature. *Nano Research* **2011**, *4* (12), 1215–1222. https://doi.org/10.1007/s12274-011-0172-3.

[72] Kwon, J.; Suh, Y. D.; Lee, J.; Lee, P.; Han, S.; Hong, S.; Yeo, J.; Lee, H.; Ko, S. H. Recent Progress in Silver Nanowire Based Flexible/Wearable Optoelectronics. *Journal of Materials Chemistry C* **2018**, *6* (28), 7445–7461. https://doi.org/10.1039/c8tc01024b.

[73] Hoffman, C. A.; Driggers, R. G. *Encyclopedia of Optical and Photonic Engineering, Second Edition*; 2015. https://doi.org/10.1081/e-eoe2.

[74] Rakić, A. D.; Djurišić, A. B.; Elazar, J. M.; Majewski, M. L. Optical Properties of Metallic Films for Vertical-Cavity Optoelectronic Devices. *Applied Optics* **1998**, *37* (22), 5271. https://doi.org/10.1364/ao.37.005271.

[75] Langley, D.; Giusti, G.; Mayousse, C.; Celle, C.; Bellet, D.; Simonato, J.-P. Flexible Transparent Conductive Materials Based on Silver Nanowire Networks:

A Review. *Nanotechnology* **2013**, *24* (45), 452001. https://doi.org/10.1088/0957-4484/24/45/452001.

[76] Wang, D.; Song, C.; Hu, Z.; Zhou, X. Synthesis of Silver Nanoparticles with Flake-like Shapes. *Materials Letters* **2005**, *59* (14-15), 1760–1763. https://doi.org/10.1016/j.matlet.2005.01.061.

[77] Chen, W.; Thoreson, M. D.; Ishii, S.; Kildishev, A. V.; Shalaev, V. M. Ultra-Thin Ultra-Smooth and Low-Loss Silver Films on a Germanium Wetting Layer. *Optics Express* **2010**, *18* (5), 5124. https://doi.org/10.1364/oe.18.005124.

[78] Gall, D. Electron Mean Free Path in Elemental Metals. *Journal of Applied Physics* **2016**, *119* (8), 085101. https://doi.org/10.1063/1.4942216.

[79] Larciprete, M. C.; Albertoni, A.; Belardini, A.; Leahu, G.; Li Voti, R.; Mura, F.; Sibilia, C.; Nefedov, I.; Anoshkin, I. V.; Kauppinen, E. I.; Nasibulin, A. G. Infrared Properties of Randomly Oriented Silver Nanowires. *Journal of Applied Physics* **2012**, *112* (8), 083503. https://doi.org/10.1063/1.4759374.

[80] Hsu, P.-C.; Liu, X.; Liu, C.; Xie, X.; Lee, H. R.; Welch, A. J.; Zhao, T.; Cui, Y. Personal Thermal Management by Metallic Nanowire-Coated Textile. *Nano Letters* **2014**, *15* (1), 365–371. https://doi.org/10.1021/nl5036572.

[81] Choe, A.; Kwon, Y.; Shin, Y.-E.; Yeom, J.; Kim, J.; Ko, H. Adaptive IR- and Water-Gating Textiles Based on Shape Memory Fibers. *ACS Appl. Mater. Interfaces* **2022**, *14* (49), 55217–55226. https://doi.org/10.1021/acsami.2c15974.

[82] Sen, L.; Wang, H.; Zhang, X.; Wang, D.; Zu, D.; Song, J.; Liu, Z.; Huang, Y.; Huang, K.; Tao, N.; Li, Z.; Bai, X.; Li, B.; Lei, M.; Yu, Z.; Wu, H. Direct Spray-Coating of Highly Robust and Transparent Ag Nanowires for Energy Saving Windows. *Nano Energy* **2019**, *62*, 111–116. https://doi.org/10.1016/j.nanoen.2019.04.071.

[83] Liu, X.; Wu, C.; Wang, X. Synthesis, Characterization, and Infrared-Emissivity Study of Ni–P–CB Nanocomposite Coatings by Electroless Process. *Journal of Coatings Technology and Research* **2010**, *7* (5), 659–664. https://doi.org/10.1007/s11998-009-9233-x.

[84] Lee, J.-Y.; Connor, S. T.; Cui, Y.; Peumans, P. Solution-Processed Metal Nanowire Mesh Transparent Electrodes. *Nano Letters* **2008**, *8* (2), 689–692. https://doi.org/10.1021/nl073296g.

[85] Atkinson, J.; Goldthorpe, I. A. Near-Infrared Properties of Silver Nanowire Networks. *Nanotechnology* **2020**, *31* (36), 365201. https://doi.org/10.1088/1361-6528/ab94de.

[86] Yamada, Y.; Yamashita, M.; Sasaki, T.; Okuzaki, H.; Otani, C. Carrier Transport of Conducting Polymer PEDOT:PSS Investigated by Temperature Dependence of THz and IR Spectra. *2014 39th International Conference on Infrared, Millimeter, and Terahertz waves (IRMMW-THz)* **2014**. https://doi.org/10.1109/irmmw-thz.2014.6956089.

[87] Deignan, G.; A. Goldthorpe, I. The Dependence of Silver Nanowire Stability on Network Composition and Processing Parameters. *RSC Advances* **2017**, *7* (57), 35590–35597. https://doi.org/10.1039/C7RA06524H.

[88] Park, B.; Bae, I.-G.; Huh, Y. H. Aligned Silver Nanowire-Based Transparent Electrodes for Engineering Polarisation-Selective Optoelectronics. *Scientific Reports* **2016**, *6* (1). https://doi.org/10.1038/srep19485.

[89] Asefnejad, A.; Khorasani; Behnamghader; Bonakdar. Manufacturing of Biodegradable Polyurethane Scaffolds Based on Polycaprolactone Using a Phase Separation Method: Physical Properties and in Vitro Assay. *International Journal of Nanomedicine* **2011**, 2375. https://doi.org/10.2147/ijn.s15586.

[90] Liu, Z.; Ban, G.; Ye, S.; Liu, W.; Liu, N.; Tao, R. Infrared Emissivity Properties of Infrared Stealth Coatings Prepared by Water-Based Technologies. *Opt. Mater. Express* **2016**, *6* (12), 3716–3716. https://doi.org/10.1364/ome.6.003716.

[91] Wang, C.; Li, G.; Xu, L.; Li, J.; Zhang, D.; Zhao, T.; Sun, R.; Zhu, P. Low Temperature Sintered Silver Nanoflake Paste for Power Device Packaging and Its Anisotropic Sintering Mechanism. *ACS applied electronic materials* **2021**, *3* (12), 5365–5373. https://doi.org/10.1021/acsaelm.1c00857.